

---

# Elevating Spectral GNNs through Enhanced Band-pass Filter Approximation

---

Guoming Li<sup>1,2</sup> Jian Yang<sup>3</sup> Shangsong Liang<sup>2</sup> Dongsheng Luo<sup>4</sup>

## Abstract

Spectral Graph Neural Networks (GNNs) have attracted great attention due to their capacity to capture patterns in the frequency domains with essential graph filters. Polynomial-based ones (namely poly-GNNs), which approximately construct graph filters with conventional or rational polynomials, are routinely adopted in practice for their substantial performances on graph learning tasks. However, previous poly-GNNs aim at achieving overall lower approximation error on different types of filters, e.g., low-pass and high-pass, but ignore a key question: *which type of filter warrants greater attention for poly-GNNs?* In this paper, we first show that poly-GNN with a better approximation for band-pass graph filters performs better on graph learning tasks. This insight further sheds light on critical issues of existing poly-GNNs, i.e., those poly-GNNs achieve trivial performance in approximating band-pass graph filters, hindering the great potential of poly-GNNs. To tackle the issues, we propose a novel poly-GNN named TrigoNet. TrigoNet constructs different graph filters with novel trigonometric polynomial, and achieves leading performance in approximating band-pass graph filters against other polynomials. By applying Taylor expansion and deserting nonlinearity, TrigoNet achieves noticeable efficiency among baselines. Extensive experiments show the advantages of TrigoNet in both accuracy performances and efficiency.

graph signal processing (GSP) (Ortega et al., 2018; Dong et al., 2020). By performing filtering operations on graph data with essential graph filters, spectral GNNs extract crucial frequency information in graph data, leading to superior performance in graph learning tasks (Zhao et al., 2019; Zeng et al., 2021; He et al., 2020; Xia et al., 2021; Fout et al., 2017; Qiu et al., 2018; Chen et al., 2019).

Despite the theoretical advantage, creating graph filters with eigen-decomposition of the graph Laplacian, especially for large graphs in real life, can be computationally expensive (Wu et al., 2021; Bo et al., 2023). Polynomial-based spectral GNNs (shortly poly-GNNs), which approximately construct graph filters with conventional or rational polynomials (Smyth, 1998; Phillips, 2003), are thereby proposed to avoid the crucial computational cost and further achieve significant performance on graph learning tasks (He et al., 2021; 2022; Wang & Zhang, 2022; Guo & Wei, 2023).

In prior studies, poly-GNNs have been developed with a uniform approach towards different graph filter types, such as low-pass and high-pass, primarily focusing on minimizing the overall approximation error across these types (He et al., 2021; 2022; Wang & Zhang, 2022). However, this approach raises a crucial, yet often overlooked question: *which type of graph filter warrants greater attention for poly-GNNs?*

Motivated by this question, in this paper, with theoretical proofs and empirical evidence, we show that poly-GNN with a better approximation ability for band-pass graph filters has better performance on graph learning tasks. This insight further unveils critical issues of existing poly-GNNs, i.e., those poly-GNNs only achieve trivial approximation performance to band-pass graph filters, which hinders the great potential of poly-GNNs. Specifically, conventional polynomials like Chebyshev polynomial (Rivlin, 2020) have proven inappropriate for approximating band-pass functions (Newman, 1979; Popov, 2011; Achieser, 2013), indicating potentially detrimental effects to the conventional poly-GNNs. On the other hand, though rational polynomial has proven capable in approximating band-pass functions (Newman, 1979; Popov, 2011), implementations of rational poly-GNNs require computation of matrix inverse, leading to unbearable computational cost. Thus, in practice, the rational poly-GNNs are approximately constructed with conventional polynomials and achieve less comparative model perfor-

## 1. Introduction

Spectral Graph Neural Networks (GNNs) are an important branch of GNNs that regard the graph data as signals on graph and process them in frequency domain (Bo et al., 2023), which are based on the mathematical framework of

---

<sup>1</sup>Independent Researcher <sup>2</sup>MBZUAI <sup>3</sup>Institute of Automation, Chinese Academy of Sciences <sup>4</sup>Florida International University. Correspondence to: Guoming Li <paskardli@outlook.com>.

mances (Levie et al., 2019; Bianchi et al., 2020).

To develop new poly-GNN with significant capability in constructing band-pass graph filters, we investigate a novel graph filter constructed with trigonometric polynomial. Although previous works in signal processing domain have verified the substantial ability of trigonometric polynomial in constructing band-pass filters (Taubin et al., 1996; Fu & Willson, 1999; Davidson et al., 2002; Gudino et al., 2008; Zahradnik & Vlcek, 2012; Zhao & Tay, 2023), such polynomial is highly overlooked in conducting poly-GNN due to nontrivial challenges in computation complexity. Precisely, constructing graph filters with trigonometric polynomial requires eigen-decomposition on graph Laplacian, which is unbearable in real-life graphs. We handle the challenge by applying Taylor expansion (Balcilar et al., 2021; Smyth, 1998; Phillips, 2003) on the trigonometric functions, making an efficient instantiation of the trigonometric graph filter. With the proposed graph filter, we further introduce a novel poly-GNN, TrigoNet. Motivated by (Rongzhe et al., 2022; Wang & Zhang, 2022), TrigoNet deserts the nonlinear component commonly used in poly-GNNs, and involves multiple linear transform (MLT), a novel mechanism that assigns individual transform matrix to each frequency component, leading to noticeable simplicity of model structure. With extensive experiments on 11 datasets, we show the advantages of TrigoNet in both efficiency and accuracy performances.

## 2. Notations and Preliminaries

In this paper, we use the boldface lowercase letters for *Vectors*, e.g.,  $\mathbf{v}$ . *Matrices* are denoted with boldface uppercase letters, e.g.,  $\mathbf{M}$ . Let  $\mathcal{G} = (\mathcal{V}, \mathcal{E}, \mathbf{X})$  denote an undirected graph  $\mathcal{G}$  with a finite node set  $\mathcal{V} = \{v_1, v_2, \dots, v_N\}$ , an edge set  $\mathcal{E} \subseteq \mathcal{V} \times \mathcal{V}$ , and a node feature matrix  $\mathbf{X} \in \mathbb{R}^{N \times F}$ , where  $F$  is dimension of node feature. Let  $\mathbf{A} \in \{0, 1\}^{N \times N}$  be the unweighted adjacency matrix of  $\mathcal{G}$  and  $\mathbf{D}$  be the diagonal matrix whose diagonal element  $D_{ii}$  is the degree of node  $v_i$ . Let  $\mathbf{L} = \mathbf{I} - \mathbf{D}^{-\frac{1}{2}} \mathbf{A} \mathbf{D}^{-\frac{1}{2}} \in \mathbb{R}^{N \times N}$  be the normalized graph Laplacian matrix of  $\mathcal{G}$ , where  $\mathbf{I}$  is the identity matrix. Let  $\mathbf{L} = \mathbf{U} \mathbf{diag}(\boldsymbol{\lambda}) \mathbf{U}^T$  be the eigen-decomposition of  $\mathbf{L}$ , where  $\mathbf{U} \in \mathbb{R}^{N \times N}$  is the matrix of eigen-vectors of  $\mathbf{L}$ ,  $\boldsymbol{\lambda} \in \mathbb{R}^N$  is the vector of the corresponding eigen-values and  $\mathbf{diag}(\boldsymbol{\lambda})$  is the diagonal matrix of  $\boldsymbol{\lambda}$ .

### 2.1. Spectral GNNs with Polynomial Filters

**Graph Signal Processing and spectral GNNs.** Graph signal processing (GSP) is defined based on the spectral graph theory (Chung, 1997) and aims to develop tools for processing data defined on graph domains (Ortega et al., 2018; Sandryhaila & Moura, 2013a; Shuman et al., 2013). Based on the analysis framework of GSP, spectral GNNs are proposed by introducing two essential concepts, i.e., graph Fourier transform (GFT) (Sandryhaila & Moura, 2013b) and

spectral graph convolution (Shi & Moura, 2019; Gama et al., 2020). Precisely, GFT and its inverse are defined as

$$\hat{\mathbf{x}} = \mathbf{U}^T \mathbf{x}, \quad \mathbf{x} = \mathbf{U} \hat{\mathbf{x}}, \quad (1)$$

where  $\mathbf{x} \in \mathbb{R}^N$  denotes a graph signal, e.g., a column of the node feature matrix  $\mathbf{X}$ , and  $\hat{\mathbf{x}} \in \mathbb{R}^N$  is the corresponding Fourier coefficients of  $\mathbf{x}$ . GFT transforms the processing of graph data from the original vertex domain to the alternative frequency domain and further leads to a novel filtering operation for processing the graph data, i.e., spectral graph convolution, which is defined below.

$$\mathbf{f} *_G \mathbf{x} = \mathbf{U} \mathbf{diag}(\mathbf{U}^T \mathbf{f}) \mathbf{U}^T \mathbf{x}. \quad (2)$$

Here,  $\mathbf{f} \in \mathbb{R}^N$  is known as the graph filter performing a filtering operation on  $\mathbf{x}$ , and  $*_G$  denotes the convolution operation. Based on the spectral graph convolution, a general framework of the spectral GNNs can be formulated as follows (Chen et al., 2021; Wu et al., 2021).

$$\mathbf{H}^{(l+1)} = \sigma^{(l)} [\mathbf{U} \mathbf{diag}(\boldsymbol{\theta}^{(l)}) \mathbf{U}^T \mathbf{H}^{(l)} \mathbf{W}^{(l)}]. \quad (3)$$

Here,  $\boldsymbol{\theta}^{(l)}$  is a parameter vector regarded as the graph filter,  $\mathbf{H}^{(l)}$  and  $\mathbf{W}^{(l)}$  is the hidden representation and weight matrix of  $l$ -th layer,  $\sigma^{(l)}$  is a function usually implemented by neural networks.

**Spectral GNNs with polynomial-based graph filters.** To avoid the complicated eigen-decomposition in Eq. 3, a special class of spectral GNNs with polynomial-based graph filters has been proposed. Such poly-GNNs achieve approximate construction of graph filter  $\boldsymbol{\theta}$  with polynomial approximation, leading to an efficient model paradigm with only sums and products of matrices. Specifically, based on the type of involved polynomials, existing works can be broadly divided into two classes, i.e., *conventional* (He et al., 2021; 2022; Wang & Zhang, 2022; Guo & Wei, 2023) and *rational* (Chen et al., 2018; Li et al., 2019; Levie et al., 2019; Bianchi et al., 2020).

Spectral GNNs with *conventional* polynomials involve conventional polynomials, e.g., Chebyshev polynomial (Rivlin, 2020), into the construction of the graph filter  $\boldsymbol{\theta}$  as follows:

$$\boldsymbol{\theta}^{(l)} = \sum_{k=0}^K \gamma_k^{(l)} T_k(\boldsymbol{\lambda}), \quad (4)$$

where  $T_k(\cdot)$  denotes the  $k$ -th term of polynomial, and  $\gamma_k^{(l)}$  is the coefficient of  $T_k$ . Thus, the spectral GNNs with conventional polynomials are formulated as below:

$$\mathbf{H}^{(l+1)} = \sigma^{(l)} \left[ \sum_{k=0}^K \gamma_k^{(l)} T_k(\mathbf{L}) \mathbf{H}^{(l)} \mathbf{W}^{(l)} \right]. \quad (5)$$

With only sums and products of matrices in Eq. 5, the computation paradigm of these GNNs is simple and efficient.

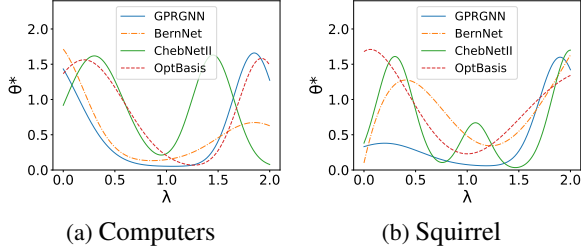


Figure 1: Graph Filters learned on Computers and Squirrel.

Spectral GNNs with *rational* polynomial conduct filter  $\theta$  with rational polynomial as follows:

$$\theta^{(l)} = \frac{\sum_{k=0}^K \alpha_k^{(l)} \lambda^k}{\sum_{k=0}^K \beta_k^{(l)} \lambda^k}, \quad (6)$$

where  $\alpha^{(l)}$  and  $\beta^{(l)}$  denote the coefficient of numerator polynomial and denominator polynomial, respectively. Thus, the relevant spectral GNNs are formulated as below:

$$\mathbf{H}^{(l+1)} = \sigma^{(l)} \left( \frac{\sum_{k=0}^K \alpha_k^{(l)} \mathbf{L}^k}{\sum_{k=0}^K \beta_k^{(l)} \mathbf{L}^k} \mathbf{H}^{(l)} \mathbf{W}^{(l)} \right). \quad (7)$$

Since matrix inverse operation in Eq. 7 is time-consuming, existing rational-based methods generally adopt approximations rather than exact implementations (Levie et al., 2019; Chen et al., 2018; Bianchi et al., 2020).

### 3. Important Role of Band-pass Graph Filters for Poly-GNNs

In this section, with empirical and theoretical analysis, we show that poly-GNN with a better ability to approximate band-pass graph filters has better model performance, and point out issues of existing poly-GNNs. We start with the definition of band-pass filter (G.Proakis, 1975):

**Definition 3.1.** Continuous filter  $f : [a, b] \mapsto \mathbb{R}$  is band-pass if  $f$  achieves non-zero on  $[c, d] \subset [a, b]$  and 0 on others.

**Empirical observations.** Recently works (He et al., 2021; Li et al., 2022; Guo et al., 2023; He et al., 2022) have shown that graph filters learned on real-world datasets are generally band-pass or sum of band-pass type. Specifically, in Figure 1, we show the graph filters learned by 4 SOTA poly-GNNs, i.e., GPRGNN (Chien et al., 2021), BernNet (He et al., 2021), ChebNetII (He et al., 2022) and OptBasisGNN (Guo & Wei, 2023), on Computers (homophilic) and Squirrel (heterophilic) datasets, where each of them is band-pass and the sum of band-pass type. Those results indicate the significance of band-pass graph filters for poly-GNNs.

Next, we perform more intuitive evidence to determine the relation between band-pass graph filters and poly-GNNs. We conduct numerical experiments of approximating different band-pass functions with 5 polynomials. We show

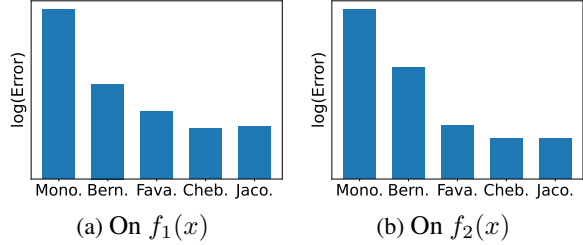

 Figure 2: Log approximation error on two band-pass functions:  $f_1(x) = |\sin(\pi x)|$  and  $f_2(x) = \exp(-10(x-1)^2)$ .

Table 1: Accuracy of SOTA poly-GNNs on 4 datasets. For each poly-GNN, we show both the model name and polynomial name corresponding to Figure 2.

Method	Cite.	Comp.	Cham.	Squi.
(Mono)GPRGNN	78.15 $\pm$ 1.78	90.05 $\pm$ 0.68	65.81 $\pm$ 2.57	51.38 $\pm$ 1.70
(Bern)BernNet	78.03 $\pm$ 1.32	90.12 $\pm$ 0.72	68.37 $\pm$ 1.87	53.23 $\pm$ 1.23
(Fava)OptBasis	78.38 $\pm$ 1.18	<b>90.27<math>\pm</math>1.03</b>	72.48 $\pm$ 2.15	57.73 $\pm$ 1.41
(Cheb)ChebNetII	<b>78.47<math>\pm</math>1.12</b>	90.15 $\pm$ 0.73	<b>73.31<math>\pm</math>1.34</b>	<b>58.12<math>\pm</math>1.69</b>
(Jaco)JacobiConv	78.33 $\pm$ 1.15	90.19 $\pm$ 0.59	72.53 $\pm$ 1.65	56.72 $\pm$ 1.54

approximation error on 2 band-pass functions in Figure 2 and more results in Appendix B. On the other hand, we show the performance (accuracy) of corresponding poly-GNNs on 4 real-life datasets in Table 1. Note that we dismiss rational cases for fairness since implementations of rational poly-GNNs (Levie et al., 2019; Bianchi et al., 2020) are approximated with conventional polynomials.

Results show that poly-GNN with a better ability in approximating band-pass graph filters has better results on graph datasets. We further compute the average rank for the results above and model the relation between Table 1 and Figure 2 with *Spearman Correlation Coefficient* (Venables, 2013). As shown in Table 2, the coefficient  $\rho$  is 0.9, indicating the strong relationship between approximation ability to band-pass graph filters and poly-GNN performance.

 Table 2: Average rank (#Rk) of results in Table 1 and Figure 2. Spearman correlation Coefficient  $\rho = 0.9$  shows a strong relation between approximation error and GNN accuracy.

	GPRGNN	BernNet	OptBasis	ChebNetII	JacobConv
#Rk of Err.	5	4	3	1	2
#Rk of Acc.	4.75	4.25	2	1.5	2.5
$\rho$	<b>0.9</b>				

**Theoretical insight.** We provide theoretical insight to explain the empirical results above. Let  $T_K(\lambda; \xi)$ ,  $\lambda \in [0, 2]$ , be the  $K$ -order truncated sum of certain polynomials for approximation with parameter  $\xi$ . For example,  $T_K(\lambda; \xi) = \sum_{k=0}^K \xi_k \lambda^k$  denotes  $K$ -order monomial approximation with  $\xi_k$  as coefficient. Previous research has pointed out that the learning goal of poly-GNNs is to minimize the error between target filter  $\theta^*$  and  $T_K$  by optimizing  $\xi$ , which is

formulated as (Wang & Zhang, 2022; Guo & Wei, 2023):

$$\min_{\xi} \int_0^2 |T_K(\lambda; \xi) - \theta^*(\lambda)|^2 d\lambda. \quad (8)$$

On the other hand, based on the signal decomposition technique in signal processing (G.Proakis, 1975),  $\theta^*$  can be decomposed into the sum of  $M$  band-pass functions  $\theta_i$  as:

$$\theta^*(\lambda) = \sum_{i=1}^M \theta_i(\lambda), \theta_i(\lambda)\theta_j(\lambda) \equiv 0, \lambda \in [0, 2]. \quad (9)$$

The  $\theta_i$  here can be arbitrary band-pass functions satisfying the conditions. A special case is decomposing  $\theta^*$  on each wave crest, where each crest is taken as a  $\theta_i$ . Thus, based on the equations above, we introduce a theorem on approximation error as follows:

**Theorem 3.2. (Bounded error)** *Let  $\theta^*(\lambda)$  be the target filter that is formulated as the sum of band-pass:  $\theta^*(\lambda) = \sum_{i=1}^M \theta_i^*(\lambda)$ ,  $T_K(\lambda; \xi)$  be the  $K$ -order truncated sum of certain polynomials used for approximating  $\theta^*(\lambda)$ . Suppose the minimal approximation error as Eq. 8 to  $\theta^*(\lambda)$  is  $\epsilon$ , and minimal approximation error to  $\theta_i^*(\lambda)$  is  $\epsilon_i$ ,  $i = 1, 2, \dots, M$ , we have  $\epsilon \leq M \sum_{i=1}^M \epsilon_i$ .*

The proof is in Appendix A.1. Theorem 3.2 demonstrates that the approximation error to the target  $\theta^*$  is upper bounded by the approximation error to band-pass filters. That is, a better ability to approximate band-pass graph filters will result in better approximation to the target filter, which means better performance of poly-GNNs.

**Drawbacks of existing works.** Based on the discussions above, critical drawbacks of existing poly-GNNs are unveiled. Although existing poly-GNNs have achieved overall lower approximation error on different types of filters, their approximation abilities to the important band-pass filters are trivial. On one hand, while those poly-GNNs with conventional polynomials have achieved substantial results (Wang & Zhang, 2022; Guo & Wei, 2023), conventional polynomials have proven inappropriate for approximating band-pass type filters (Newman, 1979; Popov, 2011; Achieser, 2013), indicating potentially detrimental effects to relevant poly-GNNs. On the other hand, while rational polynomial can achieve significant approximation to band-pass functions (Isufi et al., 2017; Rimleascaia & Isufi, 2020; Patanè, 2023; Newman, 1979; Popov, 2011; Achieser, 2013), implementing rational poly-GNNs faces critical challenge: the matrix inverse computation in Eq. 7 is exceedingly time-consuming and even unachievable on large graphs (Hu et al., 2020). Thus, practical implementations of rational poly-GNNs are approximately constructed with conventional polynomials, and achieve only trivial results. To sum up, those issues hinder the great potential of poly-GNNs, motivating us to propose our TrigoNet that possesses leading ability in approximating band-pass filters.

## 4. TrigoNet Model

In this section, we introduce our TrigoNet model. Starting with showing overall model in Figure 3, we thoroughly introduce each component of the proposed TrigoNet.

### 4.1. Graph Filter with Trigonometric Polynomial

Inspired by previous research of constructing band-pass filters in traditional signal processing (Taubin et al., 1996; Fu & Willson, 1999; Davidson et al., 2002; Gudino et al., 2008; Zahradnik & Vlcek, 2012; Zhao & Tay, 2023), we construct the graph filter of TrigoNet with trigonometric polynomial (Zygmund & Fefferman, 2003; Sharma & Varma, 1965), while the rationality of such construction is guaranteed by the following proposition:

**Proposition 4.1. (Local trigonometric expansion)** *For any real function  $f : [a, b] \rightarrow \mathbb{R}$ , ( $a < b$ ) with a finite number of discontinuities of the first kind, its expansion with trigonometric polynomial can be formulated as below:*

$$f(x) = \gamma + \sum_{k=1}^{+\infty} [\alpha_k \sin(k\omega x) + \beta_k \cos(k\omega x)]. \quad (10)$$

Here, the arbitrary real number  $\omega \in \left(0, \frac{2\pi}{b-a}\right)$  denotes the fundamental frequency of trigonometric polynomial, and also one of hyper-parameters of TrigoNet;  $\gamma$ ,  $\{\alpha_k; k \in \mathbb{N}^+\}$  and  $\{\beta_k; k \in \mathbb{N}^+\}$  denote the polynomial coefficients.

We defer the proof to Appendix A.2. Based on the proposition above, we propose a learnable graph filter  $\theta_{\text{Trigo}}$  formulated as follows.

$$\theta_{\text{Trigo}}(\lambda) = \psi_{\gamma} \cdot \mathbf{1} + \sum_{k=1}^K [\psi_{\alpha,k} \sin(k\omega\lambda) + \psi_{\beta,k} \cos(k\omega\lambda)]. \quad (11)$$

Here,  $\mathbf{1} \in \mathbb{R}^N$  is a vector whose elements are all 1;  $K$  is the order of truncated trigonometric polynomial;  $\psi_{\gamma}$ ,  $\{\psi_{\alpha,k}; k \in \mathbb{N}^+\}$  and  $\{\psi_{\beta,k}; k \in \mathbb{N}^+\}$  are parameters.

**Effective instantiation of  $\theta_{\text{Trigo}}(\lambda)$ .** Similar to other polynomial methods (Hildebrand, 1987), to avoid the intractable sum of infinite series in Eq. 10, we use  $K$ -order truncation to achieve an approximate instantiation of  $\theta_{\text{Trigo}}(\lambda)$ . Though being truncated, its substantial ability in function approximation is guaranteed by the proposition as below:

**Proposition 4.2. (Vanishing coefficients)** *Given a  $f(x)$  as Eq. 10, its coefficients  $\alpha_k$  and  $\beta_k$  satisfies*

$$\lim_{k \rightarrow +\infty} \alpha_k = 0, \quad \lim_{k \rightarrow +\infty} \beta_k = 0. \quad (12)$$

We defer the proof to Appendix A.3. The proposition above theoretically proves that those polynomial terms with large  $k$  are associated with small coefficients (weights), indicating

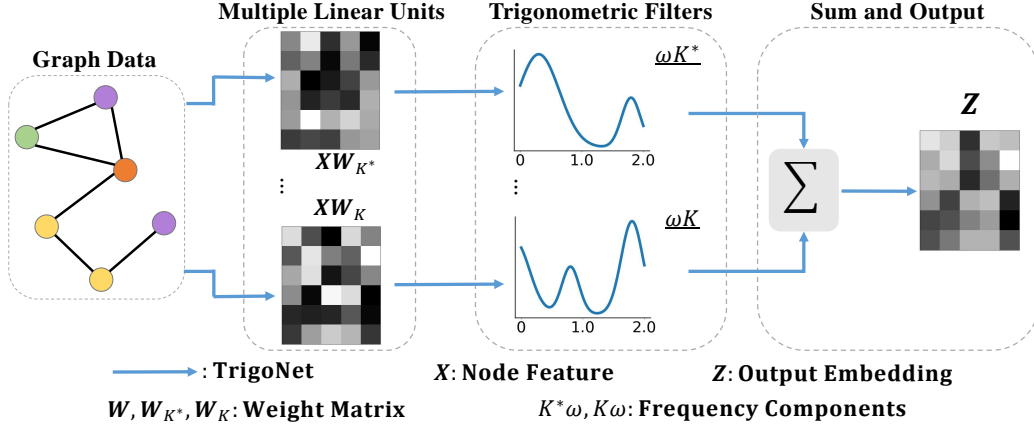
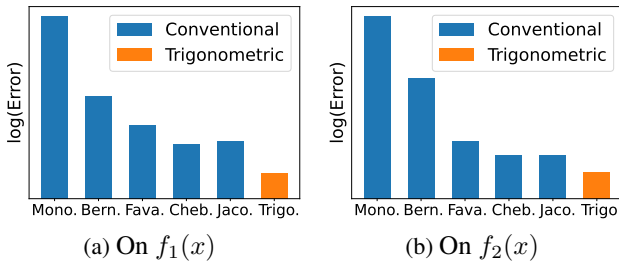


Figure 3: Overall framework of TrigoNet.


 Figure 4: Log approximation error to  $f_1(x)$  and  $f_2(x)$ .

that high order terms are “unimportant” for function construction. Thus, the  $\theta_{\text{Trigo}}$  with  $K$ -order truncated trigonometric polynomial can still maintain substantial approximation ability. We empirically verified our statement with numerical experiments. As shown in Figure 4, the truncated  $\theta_{\text{Trigo}}$  achieves leading performance against other polynomials in approximating band-pass functions. More results are deferred to Appendix B. Furthermore, since  $\sin(k\omega\lambda)$  and  $\cos(k\omega\lambda)$  will approximately approach constants, i.e., 0 and 1, when  $k\omega$  is small, we merge those polynomial terms with small  $k\omega$  into the constant part  $\psi_\gamma \cdot 1$  and achieve a more flexible instantiation to  $\theta_{\text{Trigo}}$  as follows:

$$\theta_{\text{Trigo}}(\lambda) = \psi_\gamma \cdot 1 + \sum_{k=K^*}^K [\psi_{\alpha,k} \sin(k\omega\lambda) + \psi_{\beta,k} \cos(k\omega\lambda)], \quad (13)$$

where  $K^*$  and  $K$  are both hyper-parameters.

## 4.2. Implementation with Taylor Expansion

According to Eq. 3, formal instantiation of spectral GNN requires time-consuming eigen-decomposition on  $L$ , leading to unexpected computational complexity to TrigoNet. Different to other existing methods, we handle this issue through conducting Taylor expansion (Balcilar et al., 2021; Smyth, 1998; Phillips, 2003) on the trigonometric functions in Eq. 13. Taylor expansion is an approximation method that performs high efficiency and accuracy in approximating

different functions in a local interval (Nilsson et al., 2014; Lukas et al., 2016; Zhiwei & Wei, 2017; Moral & Niclas, 2018; Peng et al., 2019; Ioannis et al., 2023), while previous works have empirically proved that such approximation technique could achieve efficient and accurate approximation to trigonometric functions (James & Michael, 1999; Lee & Burgess, 2003; Brunelli et al., 2009). Since instantiation of  $\theta_{\text{Trigo}}(\lambda)$  can be effectively achieved with finite number of  $k$  based on Proposition 4.2, applying Taylor expansion is thereby reasonable. With applying Taylor expansion, the right side of Eq. 13 can be reformulated as below:

$$\psi_\gamma \cdot 1 + \sum_{k=K^*}^K [\psi_{\alpha,k} T_{\sin}^{(k)}(\lambda) + \psi_{\beta,k} T_{\cos}^{(k)}(\lambda)], \quad (14)$$

where  $T_{\sin}^{(k)}(\lambda)$ ,  $T_{\cos}^{(k)}(\lambda)$  denote the Taylor expansion of  $\sin(k\omega\lambda)$  and  $\cos(k\omega\lambda)$  respectively. Similar to the polynomial degree of previous poly-GNNs (Chien et al., 2021; He et al., 2021; 2022; Guo & Wei, 2023), the order of Taylor expansion will be taken as hyper-parameter.

## 4.3. Linear GNNs and Multiple Linear Transform

**Deserting nonlinearity in spectral GNNs.** Recently studies have surprisingly shown that GNNs without nonlinearity (Wu et al., 2019; Wang & Zhang, 2022; Rongzhe et al., 2022) or with nonlinear activation only in the output (Chien et al., 2021) still achieve significant results, and even surpass those with nonlinear units in many cases (the effect of nonlinearity in GNNs is discussed in (Rongzhe et al., 2022)). Motivated by this insight, we propose our TrigoNet as a linear GNN deserting nonlinearity. That is, the  $\sigma(\cdot)$  in Eq. 3 is implemented with linear transformation instead of MLP used in other methods (He et al., 2021; 2022; Guo & Wei, 2023; Bianchi et al., 2020; Chen et al., 2018), leading to a noticeable light model architecture.

**Multiple linear transform (MLT).** Inspired by the parallel paradigm of ChebNet (Defferrard et al., 2016) and

ARMA (Bianchi et al., 2020), we further introduce a novel technique named Multiple Linear Transform (MLT) that assigns an individual matrix  $\mathbf{W}_k$  to each frequency component  $k$  in Eq. 14 to perform feature transformation, making TrigoNet more flexible in paradigm.

#### 4.4. Overall Model Paradigm

With discussions in Section 4.1, 4.2 and 4.3, we show the overall formulation of TrigoNet as below:

$$\mathbf{Z} = \psi_\gamma \mathbf{X} \mathbf{W}_{\text{const}} + \sum_{k=K^*}^K [\psi_{\alpha,k} T_{\text{sin}}^{(k)}(\mathbf{L}; \omega) + \psi_{\beta,k} T_{\text{cos}}^{(k)}(\mathbf{L}; \omega)] \mathbf{X} \mathbf{W}_k, \quad (15)$$

where  $\mathbf{Z}$  denotes output of TrigoNet (node embeddings in this paper), and  $\{\mathbf{W}_{K^*}, \mathbf{W}_{K^*+1}, \dots, \mathbf{W}_K, \mathbf{W}_{\text{const}}\}$  denotes the set of transformation matrices of MLT.

Table 3: Complexity comparison.  $N$ : Num of nodes;  $F$ : Feature dimension;  $H$ : Hidden units;  $C$ : Output dimension;  $K$ : Polynomial order;  $T$ : Taylor expansion order.

Method	Computation Complexity	Param Complexity
GPRGNN	$NH(F+C) + N^2KC$	$H(F+C)$
ChebNetII	$NH(F+C) + N^2KC$	$H(F+C)$
OptBasis	$NH(F+C) + N^2KC$	$H(F+C)$
JacobiConv	$NCF + N^2KC$	$FC$
TrigoNet	$(K-K^*)(NCF + N^2TC)$	$(K-K^*)FC$

**Complexity analysis.** In Table 3, we compare TrigoNet to other 4 poly-GNNs on both computational complexity and parameter complexity. As  $N$  and  $F$  are far larger than other values, desiring nonlinearity makes TrigoNet achieve lower model complexity against most counterparts. Furthermore, though the MLT mechanism involves an additional increase in complexity, in the experiment section, we will show that TrigoNet still maintains competitive efficiency.

## 5. Experiments

In this section, we conduct node classification tasks on 11 graph datasets to evaluate the performance of our TrigoNet and investigate the effect of each component in the model.

### 5.1. Node Classification

**Datasets.** We use 5 homophilic datasets, including citation graphs: Cora, CiteSeer, PubMed (Yang et al., 2016), and the Amazon co-purchase graphs: Computers, Photo (Shchur et al., 2019). We also use 4 heterophilic datasets, including Wikipedia graphs: Chameleon and Squirrel (Rozemberczki et al., 2021), and two webpage graphs from WebKB<sup>1</sup>: Texas, Cornell. For all 9 datasets, we take 60%/20%/20%

<sup>1</sup><http://www.cs.cmu.edu/afs/cs.cmu.edu/project/theo-11/www/wwkb>

train/validation/test split ratio following (He et al., 2021; 2022; Wang & Zhang, 2022; Guo & Wei, 2023). We generate 10 random splits for each dataset and evaluate all models on the same splits, where each model is evaluated 10 times with 10 random initializations on each random split.

**Baselines and settings.** We involve 11 baseline models, including GCN (Kipf & Welling, 2017), ChebNet (Defferrard et al., 2016), APPNP (Gasteiger et al., 2019), GPRGNN (Chien et al., 2021), BernNet (He et al., 2021), CayleyNet (Levie et al., 2019), IGCN (Li et al., 2019), ARMA (Bianchi et al., 2020), and SOTA models JacobiConv (Wang & Zhang, 2022), ChebNetII (He et al., 2022) and OptBasis (Guo & Wei, 2023). We follow the same settings as (He et al., 2022; Guo & Wei, 2023) for baselines except for CayleyNet, IGCN and JacobiConv, and take the settings from original papers (Levie et al., 2019; Li et al., 2019; Wang & Zhang, 2022) for those three models. Baselines are implemented with PyG (Fey & Lenssen, 2019) or publicly released code. For TrigoNet, we follow the formulations in Eq. 15, where hyper-parameters are optimized with grid search. *Cross Entropy* is used as the loss function and Adam optimizer (Kingma & Ba, 2014) to train the models, where an early stopping 250 and a maximum of 2000 epochs are set for all datasets. More experimental details are listed in Appendix C.2.

**Results and analysis.** We report experimental results in Table 4, while **boldface letter** denotes the best result and underline denotes the second for each dataset. We further provide an evaluation of model efficiency and complexity on top-7 models in Table 5, including average training time per epoch, total training time, and number of parameters on each dataset. As shown in both tables, TrigoNet has achieved significant effectiveness with comparable efficiency among baselines. Notably, other methods achieve promising performance on only part of these datasets but perform averagely on the rest datasets. In contrast, our TrigoNet maintains leading results on all datasets with noticeable accuracy improvements over the second-best, indicating the effectiveness of our approach. Moreover, though the MLT mechanism causes an increase in model complexity, TrigoNet still maintains top-2 efficiency among baselines. We visualize the learned filters of TrigoNet in Appendix F.

### 5.2. Node Classification on Large-scale Datasets

**Datasets.** We involve two large-scale graphs: ogbn-arxiv and ogbn-papers100M (Hu et al., 2020), to evaluate the scalability of our method. For data split on large graphs, we follow the standard split (Hu et al., 2020) and evaluate each model 5 times with random initializations. Evaluation metric, training, and testing settings are same as Section 5.1.

**Baselines and settings.** We involve 10 baselines, including GCN (Kipf & Welling, 2017), GPRGNN (Chien et al.,

Table 4: Mean classification accuracy (%)  $\pm$  standard deviation of node classification results.

Method	Cora	Cite.	Pubm.	Comp.	Photo	Cham.	Squi.	Texas	Corn.
GCN	87.11 $\pm$ 0.75	77.56 $\pm$ 0.69	87.05 $\pm$ 0.62	86.25 $\pm$ 0.77	88.54 $\pm$ 0.55	54.31 $\pm$ 2.03	42.67 $\pm$ 1.81	76.73 $\pm$ 3.82	77.39 $\pm$ 4.02
ChebNet	86.79 $\pm$ 1.55	76.78 $\pm$ 1.92	88.43 $\pm$ 0.63	88.77 $\pm$ 1.22	92.55 $\pm$ 1.23	56.91 $\pm$ 2.69	43.71 $\pm$ 1.36	77.33 $\pm$ 3.67	76.72 $\pm$ 3.44
APPNP	87.79 $\pm$ 1.32	77.62 $\pm$ 1.63	88.46 $\pm$ 0.82	87.11 $\pm$ 0.93	89.43 $\pm$ 0.63	52.32 $\pm$ 1.57	46.33 $\pm$ 1.84	78.92 $\pm$ 3.45	77.13 $\pm$ 3.87
GPRGNN	88.75 $\pm$ 1.07	78.15 $\pm$ 1.78	88.76 $\pm$ 0.82	90.05 $\pm$ 0.68	93.49 $\pm$ 0.59	65.81 $\pm$ 2.57	51.38 $\pm$ 1.70	80.72 $\pm$ 3.65	79.21 $\pm$ 4.28
BernNet	88.49 $\pm$ 1.22	78.03 $\pm$ 1.32	89.47 $\pm$ 0.47	90.12 $\pm$ 0.72	92.51 $\pm$ 0.71	68.37 $\pm$ 1.87	53.23 $\pm$ 1.23	79.79 $\pm$ 3.79	78.53 $\pm$ 3.81
CayleyNet	88.13 $\pm$ 1.21	77.25 $\pm$ 1.78	87.81 $\pm$ 0.91	88.58 $\pm$ 0.60	91.69 $\pm$ 0.68	61.44 $\pm$ 1.31	49.79 $\pm$ 1.22	78.66 $\pm$ 4.52	78.16 $\pm$ 4.39
IGCN	88.21 $\pm$ 0.84	77.83 $\pm$ 1.53	87.76 $\pm$ 0.71	88.79 $\pm$ 1.09	92.26 $\pm$ 0.49	65.33 $\pm$ 1.64	50.92 $\pm$ 1.13	80.05 $\pm$ 3.81	78.73 $\pm$ 3.28
ARMA	88.69 $\pm$ 1.03	78.07 $\pm$ 1.53	88.30 $\pm$ 0.81	87.81 $\pm$ 0.54	93.13 $\pm$ 0.47	65.12 $\pm$ 1.33	51.68 $\pm$ 2.01	79.19 $\pm$ 4.12	78.81 $\pm$ 3.44
JacobiConv	89.19 $\pm$ 1.08	78.33 $\pm$ 1.15	89.19 $\pm$ 0.58	90.19 $\pm$ 0.59	94.88 $\pm$ 0.32	72.53 $\pm$ 1.65	56.72 $\pm$ 1.54	80.67 $\pm$ 3.76	79.55 $\pm$ 4.38
ChebNetII	88.72 $\pm$ 0.76	78.47 $\pm$ 1.12	88.75 $\pm$ 0.89	90.15 $\pm$ 0.73	94.30 $\pm$ 0.54	<b>73.31<math>\pm</math>1.34</b>	<b>58.12<math>\pm</math>1.69</b>	80.51 $\pm$ 3.42	79.48 $\pm$ 3.73
OptBasis	88.76 $\pm$ 1.03	78.38 $\pm$ 1.18	89.35 $\pm$ 0.63	90.27 $\pm$ 1.03	94.71 $\pm$ 0.33	72.48 $\pm$ 2.15	57.73 $\pm$ 1.41	80.82 $\pm$ 4.21	79.66 $\pm$ 3.23
TrigoNet	<b>90.07<math>\pm</math>1.33</b>	<b>78.91<math>\pm</math>1.28</b>	<b>89.93<math>\pm</math>0.59</b>	<b>91.38<math>\pm</math>0.52</b>	<b>96.03<math>\pm</math>0.65</b>	72.73 $\pm$ 1.33	57.85 $\pm$ 1.46	<b>81.53<math>\pm</math>4.02</b>	<b>80.12<math>\pm</math>3.77</b>

Table 5: Average training time per-epoch (ms) / Total training time (s) / Model parameters (K) of 8 representative models.

Method	Cora	Cite.	Pubm.	Comp.	Photo	Cham.	Squi.	Texas	Corn.
ARMA	95.8/40.2/120	97.1/35.4/266	88.2/43.1/30	104.7/69.5/92	103.3/45.1/71	92.6/43.2/139	106.6/55.4/125	94.4/31.2/102	95.3/30.9/102
GPRGNN	9.5/4.0/92	10.2/3.7/237	9.9/5.1/32	10.5/6.9/50	10.1/4.2/48	9.6/4.5/149	9.2/4.7/60	8.7/2.7/109	8.5/2.8/109
BernNet	43.3/18.1/92	46.1/15.6/237	48.8/23.1/32	55.2/23.7/50	53.3/23.2/48	50.7/21.9/149	55.5/24.3/60	54.5/14.8/109	46.8/14.7/109
ChebNetII	46.2/18.0/92	48.3/15.2/237	50.1/23.3/32	58.3/23.1/50	56.4/22.4/48	52.4/21.6/149	55.8/24.5/60	50.5/14.1/109	50.7/14.4/109
JacobiConv	11.9/4.9/10	10.8/3.9/22	11.8/6.0/2	11.4/7.5/8	10.5/4.7/6	9.4/4.4/12	9.7/4.9/5	9.2/3.0/11	9.2/3.0/11
OptBasis	45.7/17.8/92	48.7/15.4/237	49.8/23.1/32	58.9/22.9/50	53.7/23.1/48	50.9/22.4/149	57.3/24.9/60	52.8/15.4/109	51.9/15.3/109
TrigoNet	9.2/4.1/30	9.6/3.3/66	43.5/19.1/4	24.2/9.6/16	10.1/4.4/12	8.5/4.1/48	14.8/6.9/20	9.0/3.0/44	9.2/3.0/33

 Table 6: Mean classification accuracy (%)  $\pm$  standard deviation on large datasets. In particular, we fail to obtain BernNet’s result since its basis preprocessing procedure cannot finish within 48 hours on the papers100M dataset.

Method	ogbn-arxiv	ogbn-papers100M
GCN	71.73 $\pm$ 0.18	OOM
IGCN	71.66 $\pm$ 0.24	OOM
ARMA	71.71 $\pm$ 0.38	OOM
GPRGNN	71.83 $\pm$ 0.23	65.91 $\pm$ 0.28
BernNet	71.88 $\pm$ 0.21	/
SIGN	71.95 $\pm$ 0.13	65.67 $\pm$ 0.18
GBP	72.22 $\pm$ 0.16	65.24 $\pm$ 0.28
NDLS	72.22 $\pm$ 0.17	65.63 $\pm$ 0.24
ChebNetII	72.29 $\pm$ 0.23	67.17 $\pm$ 0.27
OptBasis	72.21 $\pm$ 0.26	<b>67.21<math>\pm</math>0.26</b>
TrigoNet	<b>72.36<math>\pm</math>0.22</b>	<b>67.21<math>\pm</math>0.26</b>

2021), BernNet (He et al., 2021), ChebNetII (He et al., 2022), OptBasis (Guo & Wei, 2023), ARMA (Bianchi et al., 2020), IGCN (Li et al., 2019), and three baselines designed for large graph: SIGN (Frasca et al., 2020), GBP (Chen et al., 2020) and NDLS (Zhang et al., 2021). The same baseline settings as (He et al., 2022; Guo & Wei, 2023) are used here. Specially, since large graphs are noticeably complicated, we replace MLT of TrigoNet with MLP, thereby making TrigoNet be the **same** model architecture as those counterparts (Gasteiger et al., 2019; Chien et al., 2021; He et al., 2021; 2022; Guo & Wei, 2023). More experimental details are listed in Appendix C.3.

**Results and analysis.** We report experimental results in Table 6 and provide an evaluation of time consumption of 7 representative poly-GNNs in Table 7, including average training time per-epoch, inference time and total training

time. As shown in both tables, TrigoNet outperforms all baselines with competitive time consumption, indicating both the effectiveness and efficiency of our method. Note that the **only** difference between TrigoNet and other baseline poly-GNNs, e.g., GPRGNN and ChebNetII, is the spectral graph filter when using MLP for TrigoNet. Therefore, those substantial results on large graph datasets verify the scalability of our TrigoNet.

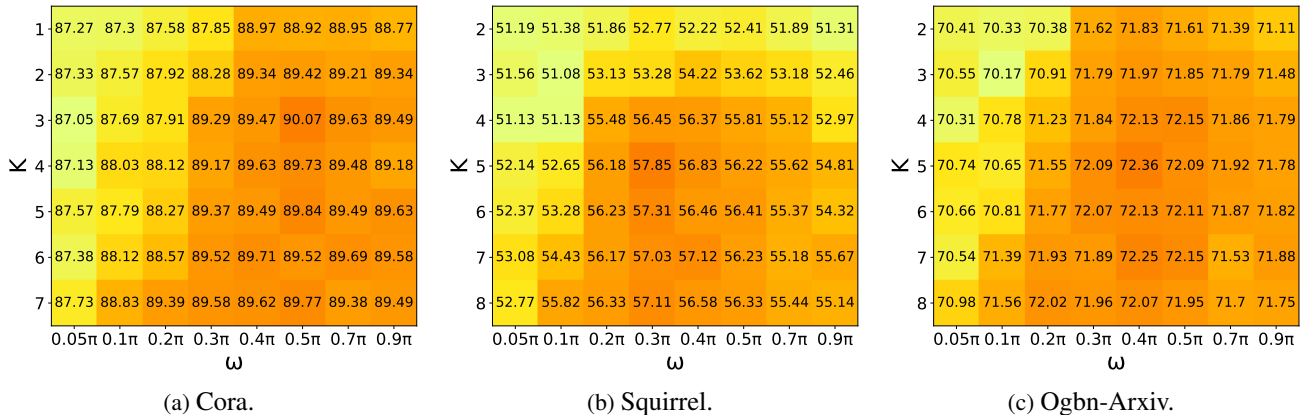
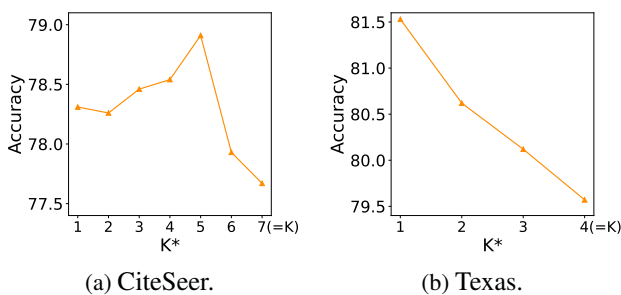
Table 7: Average training time per-epoch (s) / Inference time (s) / Total training time (hour) of 7 poly-GNNs.

Method	ogbn-arxiv	ogbn-papers100M
GCN	1.92 / 0.86 / 0.47	/
ARMA	10.6 / 4.21 / 2.67	/
GPRGNN	1.83 / 0.73 / 0.44	48.1 / 4.27 / 8.10
BernNet	1.86 / 0.76 / 0.44	/
ChebNetII	1.80 / 0.74 / 0.42	47.6 / 4.25 / 7.93
OptBasis	2.31 / 0.75 / 0.50	59.1 / 4.35 / 9.52
TrigoNet	<b>1.76 / 0.74 / 0.42</b>	<b>46.2 / 4.23 / 7.86</b>

### 5.3. Ablation Studies

We perform extensive ablation studies to analyze hyper-parameters:  $\omega$ ,  $K$ ,  $K^*$  and multiple linear transform (MLT).

**Sensitivity analysis of  $\omega$  and  $K$ .** Since  $\omega$  and  $K$  always occur as product  $K \cdot \omega$ , we investigate  $\omega$  and  $K$  jointly. Specifically, in Figure 5, we show the model sensitivity map to  $(\omega, K)$  on 3 datasets, and more results in Appendix D. Based on those relevant results, we have several insights to the  $\omega$  and  $K$ . **First**, model performance is still significant when small perturbations are added to  $\omega$  or  $K$ , indicating the certain robustness of both hyper-parameters. **Second**, while adding higher frequency (larger  $K$ ) can bring substantial


 Figure 5: Sensitivity analysis of  $\omega$  and  $K$  on Cora, Squirrel and Ogbn-Arxiv.

 Figure 6: Effect of  $K^*$  towards model performance.

performance improvements for small  $\omega$ , blindly involving high frequency cannot improve model performance but hurt it, verifying the correctness of Proposition 4.2 and Eq. 11.

**Effect of hyper-parameter  $K^*$ .** Since  $K^*$  corresponds to the flexible instantiation of  $\theta_{\text{Trigo}}$  as Eq. 13, we equivalently investigate whether such instantiation influences model performance. We use different  $K^*$  to conduct experiments, where both  $\omega$  and  $K$  are fixed to be optimal for each dataset. We show the experimental results on two datasets in Figure 6, and more results in Appendix D. Intuitively, we find two different patterns regarding the  $K^*$ : **First**,  $K^* = 5 > 1$  is the optimal choice for achieving the best performance on CiteSeer when  $\omega = 0.2\pi$ , and the model performance is relatively poor with  $K^* = 1$ . **Second**, the best result is achieved with  $K^* = 1$  on Texas when  $\omega = 0.5\pi$ , and  $K^* > 1$  will cause detrimental effect to results. These phenomena indicate that setting  $K^* > 1$  is essential for those datasets involving small  $\omega$ , and dispensable on those with large  $\omega$ , which further experimentally prove that introducing  $K^*$  into our method is effective.

**Effect of MLT mechanism.** To determine the effect of MLT mechanism, we conduct qualitative experiments to compare model performance between TrigoNet, TrigoNet removing MLT and TrigoNet using MLP. As shown in Table 8, results of using MLT are noticeably better than that with MLP on 7 datasets, while MLP makes TrigoNet achieve significant performance on large-scale datasets. According

Table 8: Comparisons between TrigoNet, removing MLT, and using MLP on all datasets.

Dataset	TrigoNet	removing MLT	using MLPs
Cora	<b>90.07</b> $\pm 1.33$	88.81 $\pm 0.92$	<u>89.37</u> $\pm 1.29$
CiteSeer	<b>78.91</b> $\pm 1.28$	78.32 $\pm 1.51$	<u>78.44</u> $\pm 1.67$
PubMed	<b>89.93</b> $\pm 0.59$	88.76 $\pm 0.77$	<u>89.61</u> $\pm 0.71$
Computers	<b>91.38</b> $\pm 0.52$	90.43 $\pm 0.81$	<u>91.02</u> $\pm 0.44$
Photo	<b>96.03</b> $\pm 0.65$	94.75 $\pm 0.53$	<u>95.73</u> $\pm 0.57$
Chameleon	<u>72.73</u> $\pm 1.33$	70.33 $\pm 1.16$	<b>73.11</b> $\pm 1.41$
Squirrel	<u>57.85</u> $\pm 1.46$	54.06 $\pm 1.81$	<b>58.72</b> $\pm 1.20$
Texas	<b>81.53</b> $\pm 4.02$	80.62 $\pm 3.77$	<u>81.20</u> $\pm 4.32$
Cornell	<b>80.12</b> $\pm 3.77$	79.59 $\pm 3.19$	<u>79.41</u> $\pm 3.91$
-arxiv	<u>71.82</u> $\pm 0.21$	71.51 $\pm 0.15$	<b>72.36</b> $\pm 0.22$
-papers100M	64.71 $\pm 0.18$	63.31 $\pm 0.20$	<b>67.21</b> $\pm 0.26$

to previous studies (Rongzhe et al., 2022; Wang & Zhang, 2022), spectral GNNs deserting nonlinearity can still capture essential information from graph data, while the nonlinearity is indispensable for complex datasets, e.g., two ogbn graphs, to learn intricate patterns. Thus, the MLT mechanism can bring significant performance improvements on most datasets, while its contributions may be inferior in special cases. Nevertheless, results achieved in Table 4 and 5 empirically prove the effectiveness of the MLT mechanism.

## 6. Conclusions

In this paper, we first show that poly-GNN with a better performance in approximating band-pass graph filters achieves better model performance, which unveils the drawbacks of existing poly-GNNs. To tackle the issues, we propose a novel poly-GNN named TrigoNet. TrigoNet constructs graph filters with novel trigonometric polynomial, and can achieve leading performance in approximating complicated band-pass graph filters against other polynomials. TrigoNet is noticeably efficient by applying Taylor expansion and deserting nonlinearity, and achieves further improvements with applying Multiple Linear Transform technique. Extensive experiments show that TrigoNet outperforms SOTA methods, verifying the correctness of our statement.

## Impact Statements

This paper presents work whose goal is to advance the field of Machine Learning. There are many potential societal consequences of our work, none of which we feel must be specifically highlighted here.

## References

- Achieser, N. I. Theory of approximation. Courier Corporation, 2013.
- Balcilar, M., Renton, G., Héroux, P., Gaüzère, B., Adam, S., and Honeine, P. Analyzing the expressive power of graph neural networks in a spectral perspective. In International Conference on Learning Representations, 2021. URL <https://openreview.net/forum?id=-qh0M9XWxnv>.
- Bianchi, F. M., Grattarola, D., Livi, L., and Alippi, C. Graph neural networks with convolutional arma filters. IEEE Transactions on Pattern Analysis and Machine Intelligence, 44(7):3496–3507, 2020. doi: 10.1109/TPAMI.2021.3054830.
- Bo, D., Wang, X., Liu, Y., Fang, Y., Li, Y., and Shi, C. A survey on spectral graph neural networks, 2023.
- Bochner, S. and Chandrasekharan, K. Fourier transforms. The Mathematical Gazette, 35(312):140–141, 1951. doi: 10.2307/3609365.
- Brunelli, C., Berg, H., and Guevorkian, D. Approximating sine functions using variable-precision taylor polynomials. In 2009 IEEE Workshop on Signal Processing Systems, pp. 57–62, 2009. doi: 10.1109/SIPS.2009.5336225.
- Chen, M., Wei, Z., Ding, B., Li, Y., Yuan, Y., Du, X., and Wen, J.-R. Scalable graph neural networks via bidirectional propagation. In Advances in Neural Information Processing Systems, volume 33, pp. 14556–14566. Curran Associates, Inc., 2020. URL [https://proceedings.neurips.cc/paper\\_files/paper/2020/file/a7789ef88d599b8df86bbe632b2994d-Paper.pdf](https://proceedings.neurips.cc/paper_files/paper/2020/file/a7789ef88d599b8df86bbe632b2994d-Paper.pdf).
- Chen, Z., Chen, F., Lai, R., Zhang, X., and Lu, C.-T. Rational neural networks for approximating graph convolution operator on jump discontinuities. In 2018 IEEE International Conference on Data Mining (ICDM), pp. 59–68, 2018. doi: 10.1109/ICDM.2018.00021.
- Chen, Z., Li, L., and Bruna, J. Supervised community detection with line graph neural networks. In International Conference on Learning Representations, 2019. URL <https://openreview.net/forum?id=H1g0Z3A9Fm>.
- Chen, Z., Chen, F., Zhang, L., Ji, T., Fu, K., Zhao, L., Chen, F., Wu, L., Aggarwal, C., and Lu, C.-T. Bridging the gap between spatial and spectral domains: A survey on graph neural networks, 2021.
- Chien, E., Peng, J., Li, P., and Milenkovic, O. Adaptive universal generalized pagerank graph neural network. In International Conference on Learning Representations, 2021. URL <https://openreview.net/forum?id=n6jl7fLxrP>.
- Chihara, T. S. An introduction to orthogonal polynomials. Courier Corporation, 2011.
- Chung, F. Spectral Graph Theory, volume 92. CBMS Regional Conference Series in Mathematics, 1997. ISBN 978-0-8218-0315-8. doi: /10.1090/cbms/092.
- Davidson, T., Luo, Z.-Q., and Sturm, J. Linear matrix inequality formulation of spectral mask constraints with applications to fir filter design. IEEE Transactions on Signal Processing, 50(11):2702–2715, 2002. doi: 10.1109/TSP.2002.804079.
- De Boor, C. and Ron, A. On multivariate polynomial interpolation. Constructive Approximation, 6:287–302, 1990.
- Defferrard, M., Bresson, X., and Vandergheynst, P. Convolutional neural networks on graphs with fast localized spectral filtering. In Lee, D., Sugiyama, M., Luxburg, U., Guyon, I., and Garnett, R. (eds.), Advances in Neural Information Processing Systems, volume 29. Curran Associates, Inc., 2016.
- Dong, X., Thanou, D., Toni, L., Bronstein, M., and Frossard, P. Graph signal processing for machine learning: A review and new perspectives. IEEE Signal Processing Magazine, 37(6):117–127, 2020. doi: 10.1109/MSP.2020.3014591.
- Fey, M. and Lenssen, J. E. Fast graph representation learning with pytorch geometric, 2019. URL <https://arxiv.org/abs/1903.02428>.
- Fout, A., Byrd, J., Shariat, B., and Ben-Hur, A. Protein interface prediction using graph convolutional networks. In Advances in Neural Information Processing Systems, volume 30. Curran Associates, Inc., 2017. URL <https://proceedings.neurips.cc/paper/2017/file/f507783927f2ec2737ba40afbd17efb5-Paper.pdf>.
- Frasca, F., Rossi, E., Eynard, D., Chamberlain, B., Bronstein, M., and Monti, F. Sign: Scalable inception graph neural networks, 2020.

- Fu, D. and Willson, A. Design of an improved interpolation filter using a trigonometric polynomial. In 1999 IEEE International Symposium on Circuits and Systems (ISCAS), volume 4, pp. 363–366 vol.4, 1999. doi: 10.1109/ISCAS.1999.780017.
- Funaro, D. Polynomial approximation of differential equations, volume 8. Springer Science & Business Media, 2008.
- Gama, F., Isufi, E., Leus, G., and Ribeiro, A. Graphs, convolutions, and neural networks: From graph filters to graph neural networks. IEEE Signal Processing Magazine, 37(6):128–138, 2020. doi: 10.1109/MSP.2020.3016143.
- Gasca, M. and Sauer, T. Polynomial interpolation in several variables. Advances in Computational Mathematics, 12: 377–410, 2000.
- Gasteiger, J., Bojchevski, A., and Günnemann, S. Predict then propagate: Graph neural networks meet personalized pagerank. In International Conference on Learning Representations, 2019. URL <https://openreview.net/forum?id=H1gL-2A9Ym>.
- G.Proakis, J. Digital signal processing. IEEE Transactions on Acoustics, Speech, and Signal Processing, 23(4):392–394, 1975. doi: 10.1109/TASSP.1975.1162707.
- Gudino, L. J., Rodrigues, J. X., and Jagadeesha, S. N. Linear phase fir filter for narrow-band filtering. In 2008 International Conference on Communications, Circuits and Systems, pp. 776–779, 2008. doi: 10.1109/ICCCAS.2008.4657886.
- Guo, J., Huang, K., Yi, X., and Zhang, R. Graph neural networks with diverse spectral filtering. In Proceedings of the ACM Web Conference 2023, pp. 306–316, New York, NY, USA, 2023. Association for Computing Machinery. ISBN 9781450394161. doi: 10.1145/3543507.3583324. URL <https://doi.org/10.1145/3543507.3583324>.
- Guo, Y. and Wei, Z. Graph neural networks with learnable and optimal polynomial bases. In Krause, A., Brunskill, E., Cho, K., Engelhardt, B., Sabato, S., and Scarlett, J. (eds.), Proceedings of the 40th International Conference on Machine Learning, volume 202 of Proceedings of Machine Learning Research, pp. 12077–12097. PMLR, 23–29 Jul 2023. URL <https://proceedings.mlr.press/v202/guo23i.html>.
- He, M., Wei, Z., Huang, Z., and Xu, H. Bernnet: Learning arbitrary graph spectral filters via bernstein approximation. In Beygelzimer, A., Dauphin, Y., Liang, P., and Vaughan, J. W. (eds.), Advances in Neural Information Processing Systems, 2021. URL [https://openreview.net/forum?id=WigDnV-\\_Gq](https://openreview.net/forum?id=WigDnV-_Gq).
- He, M., Wei, Z., and Wen, J.-R. Convolutional neural networks on graphs with chebyshev approximation, revisited. In Oh, A. H., Agarwal, A., Belgrave, D., and Cho, K. (eds.), Advances in Neural Information Processing Systems, 2022. URL <https://openreview.net/forum?id=jxPJ4QA0KAb>.
- He, X., Deng, K., Wang, X., Li, Y., Zhang, Y., and Wang, M. Lightgcn: Simplifying and powering graph convolution network for recommendation, 2020. URL <https://arxiv.org/abs/2002.02126>.
- Hildebrand, F. B. Introduction to numerical analysis. Courier Corporation, 1987.
- Hoskins, R. F. Delta functions: Introduction to generalised functions. Horwood Publishing, 2009. ISBN 978-1-904275-39-8.
- Hu, W., Fey, M., Zitnik, M., Dong, Y., Ren, H., Liu, B., Catasta, M., and Leskovec, J. Open graph benchmark: Datasets for machine learning on graphs. In Advances in Neural Information Processing Systems, volume 33, pp. 22118–22133, 2020. URL [https://proceedings.neurips.cc/paper\\_files/paper/2020/file/fb60d411a5c5b72b2e7d3527cfc84fd0-Paper.pdf](https://proceedings.neurips.cc/paper_files/paper/2020/file/fb60d411a5c5b72b2e7d3527cfc84fd0-Paper.pdf).
- Ioannis, K., Lazaros, M., and Christos, V. Assessing the chaos strength of taylor approximations of the sine chaotic map. Nonlinear Dynamics, 111:2755–2778, 2023. doi: 10.1007/s11071-022-07929-y.
- Isufi, E., Loukas, A., Simonetto, A., and Leus, G. Autoregressive moving average graph filtering. IEEE Transactions on Signal Processing, 65(2):274–288, 2017. doi: 10.1109/TSP.2016.2614793.
- James, E. S. and Michael, J. S. The symmetric table addition method for accurate function approximation. Journal of VLSI signal processing systems for signal, image and video technology, 21:167–177, 1999. doi: 10.1023/A:1008004523235.
- Kingma, D. P. and Ba, J. Adam: A method for stochastic optimization, 2014. URL <https://arxiv.org/abs/1412.6980>.
- Kipf, T. N. and Welling, M. Semi-supervised classification with graph convolutional networks. In International Conference on Learning Representations, 2017. URL <https://openreview.net/forum?id=SJU4ayYgl>.
- Lee, B. and Burgess, N. Some results on taylor-series function approximation on fpga. In The Thirty-Seventh Asilomar Conference on Signals, Systems and

- Computers, 2003, volume 2, pp. 2198–2202, 2003. doi: 10.1109/ACSSC.2003.1292370.
- Levie, R., Monti, F., Bresson, X., and Bronstein, M. M. Caylennets: Graph convolutional neural networks with complex rational spectral filters. IEEE Transactions on Signal Processing, 67(1):97–109, 2019. doi: 10.1109/TSP.2018.2879624.
- Li, M., Guo, X., Wang, Y., Wang, Y., and Lin, Z. G<sup>2</sup>CN: Graph Gaussian convolution networks with concentrated graph filters. In Chaudhuri, K., Jegelka, S., Song, L., Szepesvari, C., Niu, G., and Sabato, S. (eds.), Proceedings of the 39th International Conference on Machine Learning, volume 162 of Proceedings of Machine Learning Research, pp. 12782–12796. PMLR, Jul 2022. URL <https://proceedings.mlr.press/v162/li22h.html>.
- Li, Q., Wu, X.-M., Liu, H., Zhang, X., and Guan, Z. Label efficient semi-supervised learning via graph filtering. In Proceedings of the IEEE/CVF Conference on Computer Vision and Pattern Recognition (CVPR), June 2019.
- Litvinov, G. Approximate construction of rational approximations and the effect of error autocorrection. applications, 2001.
- Lorentz, G. G. Bernstein polynomials. American Mathematical Soc., 2013. ISBN 978-0-8218-7558-2.
- Lukas, E., Norbert, J. M., and Yong, Z. Accurate and efficient computation of nonlocal potentials based on gaussian-sum approximation. Journal of Computational Physics, 327:629–642, 2016. doi: 10.1016/j.jcp.2016.09.045.
- Mason, J. Some properties and applications of chebyshev polynomial and rational approximation. In Rational Approximation and Interpolation: Proceedings of the United Kingdom-United States Conference held at Tampa, Florida, December 12–16, 1983, pp. 27–48. Springer, 2006.
- Moral, P. D. and Niclas, A. A taylor expansion of the square root matrix function. Journal of Mathematical Analysis and Applications, 465(1):259–266, 2018. doi: 10.1016/j.jmaa.2018.05.005.
- Newman, D. J. Approximation with rational functions. Number 41. American Mathematical Soc., 1979.
- Nilsson, P., Shaik, A. U. R., Gangarajiah, R., and Hertz, E. Hardware implementation of the exponential function using taylor series. In 2014 NORCHIP, pp. 1–4, 2014. doi: 10.1109/NORCHIP.2014.7004740.
- Ortega, A., Frossard, P., Kovačević, J., Moura, J. M. F., and Vandergheynst, P. Graph signal processing: Overview, challenges, and applications. Proceedings of the IEEE, 106(5):808–828, 2018. doi: 10.1109/JPROC.2018.2820126.
- Papp, D. and Alizadeh, F. Shape-constrained estimation using nonnegative splines. Journal of Computational and Graphical Statistics, 23(1):211–231, 2014.
- Patanè, G. Fourier-based and rational graph filters for spectral processing. IEEE Transactions on Pattern Analysis and Machine Intelligence, 45(6):7063–7074, 2023. doi: 10.1109/TPAMI.2022.3177075.
- Peng, C., Umberto, V., and Omar, G. Taylor approximation and variance reduction for pde-constrained optimal control under uncertainty. Journal of Computational Physics, 385:163–186, 2019. doi: 10.1016/j.jcp.2019.01.047.
- Phillips, G. M. Interpolation and approximation by polynomials, volume 14. Springer New York, 2003. ISBN 978-0-387-00215-6. doi: 10.1007/b97417.
- Popov, V. A. Rational approximation of real functions. Number 28. Cambridge University Press, 2011.
- Qiu, J., Tang, J., Ma, H., Dong, Y., Wang, K., and Tang, J. Deepinf: Social influence prediction with deep learning. In Proceedings of the 24th ACM SIGKDD International Conference on Knowledge Discovery and Data Mining (KDD’18), 2018.
- Rimleascaia, O. and Isufi, E. Rational chebyshev graph filters. In 2020 54th Asilomar Conference on Signals, Systems, and Computers, pp. 736–740, 2020. doi: 10.1109/IEEECONF51394.2020.9443317.
- Rivlin, T. J. Chebyshev polynomials. Courier Dover Publications, 2020.
- Rongzhe, W., Haoteng, Y., Junteng, J., Benson, A. R., and Pan, L. Understanding non-linearity in graph neural networks from the bayesian-inference perspective. In Advances in Neural Information Processing Systems, 2022. URL <https://openreview.net/forum?id=Xt9smkoTgQf>.
- Rozemberczki, B., Allen, C., and Sarkar, R. Multi-scale attributed node embedding. Journal of Complex Networks, 9(2), 05 2021. doi: 10.1093/comnet/cnab014. URL <https://doi.org/10.1093/comnet/cnab014>.
- Sandryhaila, A. and Moura, J. M. F. Discrete signal processing on graphs. IEEE Transactions on Signal Processing, 61(7):1644–1656, 2013a. doi: 10.1109/TSP.2013.2238935.

- Sandryhaila, A. and Moura, J. M. F. Discrete signal processing on graphs: Graph fourier transform. In 2013 IEEE International Conference on Acoustics, Speech and Signal Processing, pp. 6167–6170, 2013b. doi: 10.1109/ICASSP.2013.6638850.
- Sharma, A. and Varma, A. K. Trigonometric interpolation. Duke Mathematical Journal, 32(2):341–357, 1965. doi: 10.1215/S0012-7094-65-03235-7. URL <https://doi.org/10.1215/S0012-7094-65-03235-7>.
- Shchur, O., Mumme, M., Bojchevski, A., and Günnemann, S. Pitfalls of graph neural network evaluation, 2019.
- Shi, J. and Moura, J. M. Topics in graph signal processing: Convolution and modulation. In 2019 53rd Asilomar Conference on Signals, Systems, and Computers, pp. 457–461, 2019. doi: 10.1109/IEEECONF44664.2019.9049012.
- Shuman, D. I., Narang, S. K., Frossard, P., Ortega, A., and Vandergheynst, P. The emerging field of signal processing on graphs: Extending high-dimensional data analysis to networks and other irregular domains. IEEE Signal Processing Magazine, 30(3):83–98, 2013. doi: 10.1109/MSP.2012.2235192.
- Smyth, G. K. Polynomial approximation. Encyclopedia of Biostatistics, 13, 1998.
- Szeg, G. Orthogonal polynomials, volume 23. American Mathematical Soc., 1939.
- Taubin, G., Zhang, T., and Golub, G. Optimal surface smoothing as filter design. In ECCV '96, pp. 283–292. Springer Berlin Heidelberg, 1996.
- Venables, W. Modern applied statistics with S-PLUS. Springer Science and Business Media, 2013.
- Wang, X. and Zhang, M. How powerful are spectral graph neural networks. In Chaudhuri, K., Jegelka, S., Song, L., Szepesvari, C., Niu, G., and Sabato, S. (eds.), Proceedings of the 39th International Conference on Machine Learning, volume 162 of Proceedings of Machine Learning Research, pp. 23341–23362. PMLR, Jul 2022. URL <https://proceedings.mlr.press/v162/wang22am.html>.
- Wu, F., Souza, A., Zhang, T., Fifty, C., Yu, T., and Weinberger, K. Simplifying graph convolutional networks. In Proceedings of the 36th International Conference on Machine Learning, volume 97, pp. 6861–6871. PMLR, 06 2019. URL <https://proceedings.mlr.press/v97/wu19e.html>.
- Wu, Z., Pan, S., Chen, F., Long, G., Zhang, C., and Yu, P. S. A comprehensive survey on graph neural networks. IEEE Transactions on Neural Networks and Learning Systems, 32(1):4–24, 2021. doi: 10.1109/TNNLS.2020.2978386.
- Xia, L., Xu, Y., Huang, C., Dai, P., and Bo, L. Graph meta network for multi-behavior recommendation. In The 44th International ACM SIGIR Conference on Research and Development in Information Retrieval, pp. 757–766, 2021. doi: 10.1145/3404835.3462972.
- Yang, Z., Cohen, W. W., and Salakhutdinov, R. Revisiting semi-supervised learning with graph embeddings, 2016. URL <https://arxiv.org/abs/1603.08861>.
- Zahradnik, P. and Vlcek, M. Perfect decomposition narrow-band fir filter banks. IEEE Transactions on Circuits and Systems II: Express Briefs, 59(11):805–809, 2012. doi: 10.1109/TCSII.2012.2218453.
- Zeng, A., Sun, X., Yang, L., Zhao, N., Liu, M., and Xu, Q. Learning skeletal graph neural networks for hard 3d pose estimation. In 2021 IEEE/CVF International Conference on Computer Vision (ICCV), pp. 11416–11425, 2021. doi: 10.1109/ICCV48922.2021.01124.
- Zhang, W., Yang, M., Sheng, Z., Li, Y., Ouyang, W., Tao, Y., Yang, Z., and CUI, B. Node dependent local smoothing for scalable graph learning. In Advances in Neural Information Processing Systems, volume 34, pp. 20321–20332. Curran Associates, Inc., 2021. URL [https://proceedings.neurips.cc/paper\\_files/paper/2021/file/a9eb812238f753132652ae09963a05e9-Paper.pdf](https://proceedings.neurips.cc/paper_files/paper/2021/file/a9eb812238f753132652ae09963a05e9-Paper.pdf).
- Zhao, L., Peng, X., Tian, Y., Kapadia, M., and Metaxas, D. N. Semantic graph convolutional networks for 3d human pose regression. In 2019 IEEE/CVF Conference on Computer Vision and Pattern Recognition (CVPR), pp. 3420–3430, 2019. doi: 10.1109/CVPR.2019.00354.
- Zhao, R. and Tay, D. B. Minimax design of two-channel critically sampled graph qmf banks. Signal Processing, 212:109129, 2023. ISSN 0165-1684. doi: <https://doi.org/10.1016/j.sigpro.2023.109129>. URL <https://www.sciencedirect.com/science/article/pii/S0165168423002037>.
- Zhiwei, Y. and Wei, Z. Shtukas and the taylor expansion of  $l$ -functions. Annals of Mathematics, 186(3):767–911, 2017. doi: 10.4007/annals.2017.186.3.2.
- Zygmund, A. and Fefferman, R. Trigonometric Series. Cambridge Mathematical Library. Cambridge University Press, 3 edition, 2003. doi: 10.1017/CBO9781316036587.

## A. Proofs

### A.1. Proof of Theorem 3.2

**(Bounded error)** Let  $\theta^*(\lambda)$  be the target filter that can be formulated as the sum of band-pass:  $\theta^*(\lambda) = \sum_{i=1}^M \theta_i^*(\lambda)$ ,  $T_K(\lambda; \boldsymbol{\xi})$  be the  $K$ -order truncated sum of certain polynomials used for approximating  $\theta^*(\lambda)$ . Suppose the minimal approximation error as Eq. 8 to  $\theta^*(\lambda)$  is  $\epsilon$ , and minimal approximation error to  $\theta_i^*(\lambda)$  is  $\epsilon_i$ ,  $i = 1, 2, \dots, M$ , we have the inequality as below:

$$\epsilon \leq M \sum_{i=1}^M \epsilon_i. \quad (16)$$

*Proof.* To begin with, we suppose the minimal approximation error to  $\theta^*(\lambda)$  is achieved with  $T_K(\lambda; \boldsymbol{\xi}^*)$ . Similarly, we can also suppose the minimal approximation error to  $\theta_i^*(\lambda)$  is achieved with  $T_K(\lambda; \boldsymbol{\xi}_i^*)$ . Next, we start from  $\epsilon$  and have the following derivations:

$$\begin{aligned} \epsilon &= \int_0^2 |T_K(\lambda; \boldsymbol{\xi}^*) - \theta^*(\lambda)|^2 d\lambda, \\ &= \int_0^2 |T_K(\lambda; \boldsymbol{\xi}^*) - \sum_{i=1}^M \theta_i^*(\lambda)|^2 d\lambda, \\ &\leq \int_0^2 \left| \sum_{i=1}^M T_K(\lambda; \boldsymbol{\xi}_i^*) - \sum_{i=1}^M \theta_i^*(\lambda) \right|^2 d\lambda, \\ &= \int_0^2 \left| \sum_{i=1}^M [T_K(\lambda; \boldsymbol{\xi}_i^*) - \theta_i^*(\lambda)] \right|^2 d\lambda. \end{aligned} \quad (17)$$

For convenience, we denote  $[T_K(\lambda; \boldsymbol{\xi}_i^*) - \theta_i^*(\lambda)]$  as  $p_i$ , thereby deriving the Eq. 17 as below:

$$\begin{aligned} &\int_0^2 \left| \sum_{i=1}^M [T_K(\lambda; \boldsymbol{\xi}_i^*) - \theta_i^*(\lambda)] \right|^2 d\lambda, \\ &\doteq \int_0^2 \left| \sum_{i=1}^M p_i \right|^2 d\lambda, \\ &= \sum_{i=1}^M \int_0^2 |p_i|^2 d\lambda + 2 \sum_{i < j} \int_0^2 |p_i \cdot p_j| d\lambda, \\ &\leq \sum_{i=1}^M \int_0^2 |p_i|^2 d\lambda + \sum_{i < j} \int_0^2 (|p_i|^2 + |p_j|^2) d\lambda, \\ &= M \sum_{i=1}^M \int_0^2 |p_i|^2 d\lambda, \\ &= M \sum_{i=1}^M \int_0^2 |T_K(\lambda; \boldsymbol{\xi}_i^*) - \theta_i^*(\lambda)|^2 d\lambda, \\ &= M \sum_{i=1}^M \epsilon_i, \end{aligned} \quad (18)$$

and the proof is completed.  $\square$

## A.2. Proof of Proposition 4.1

**(Local trigonometric expansion)** For any real function  $f : [a, b] \rightarrow \mathbb{R}$ , ( $a < b$ ) with a finite number of discontinuities of the first kind, its expansion conducted with trigonometric polynomial is formulated as below:

$$f(x) = \gamma + \sum_{k=1}^{+\infty} [\alpha_k \sin(k\omega x) + \beta_k \cos(k\omega x)] , \quad x \in [a, b] . \quad (19)$$

Here, the arbitrary real number  $\omega \in \left(0, \frac{2\pi}{b-a}\right)$  denotes the fundamental frequency of trigonometric polynomial;  $\gamma$ ,  $\{\alpha_k; k \in \mathbb{N}^+\}$  and  $\{\beta_k; k \in \mathbb{N}^+\}$  denote the polynomial coefficients.

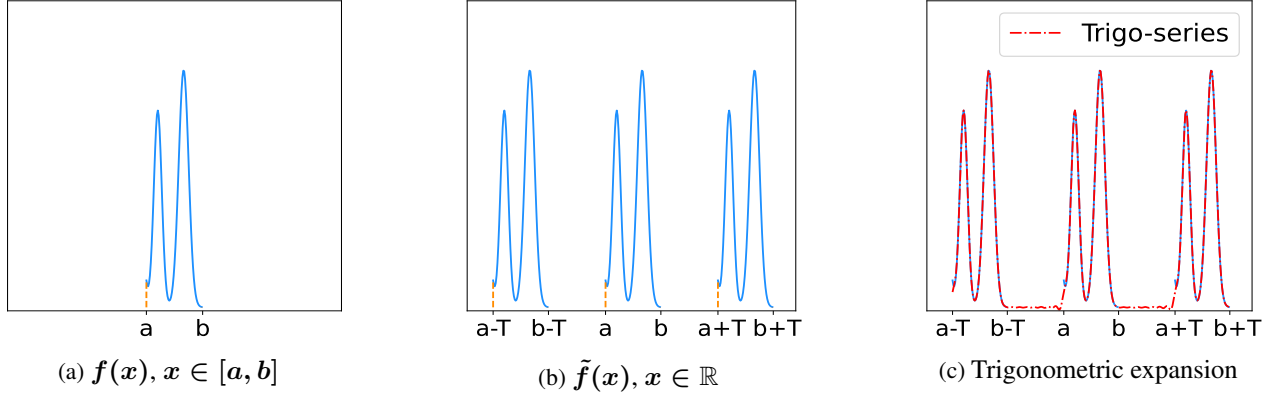


Figure 7: Intuitive display of the proof method of Proposition 4.1. Figure (a) denotes the original  $f(x)$  on the local interval  $[a, b]$ , Figures (b) shows the periodic extension of  $f(x)$ , i.e.,  $\tilde{f}(x)$ , Figure (c) shows trigonometric expansion (**truncated**) of  $f(x)$ , which is also the construction of  $f(x)$  on local interval  $[a, b]$ .

*Proof.* We first consider a periodic function  $\tilde{f}(x)$  with a period of  $T$ , where  $T$  is an arbitrary real number that satisfies  $T > b - a$ . Specially, on  $[a, a + T)$ , such  $\tilde{f}(x)$  satisfies:

$$\tilde{f}(x) = \begin{cases} f(x) , & x \in [a, b] ; \\ g(x) , & x \in (b, a + T) . \end{cases} \quad (20)$$

Here,  $g(x)$  can be **arbitrary** function with only a finite number of discontinuities of the first kind, e.g.,  $g(x) = x$ . Obviously, such a periodic function that satisfies all conditions above exists and can be easily constructed. Thus, as proposed in (Zygmund & Fefferman, 2003), the real periodic function  $\tilde{f}(x)$  can be expanded as a trigonometric series with fundamental frequency  $\omega = \frac{2\pi}{T} \in \left(0, \frac{2\pi}{b-a}\right)$ :

$$\tilde{f}(x) = \gamma + \sum_{k=1}^{+\infty} [\alpha_k \sin(k\omega x) + \beta_k \cos(k\omega x)] , \quad x \in \mathbb{R} , \quad (21)$$

where  $\gamma$ ,  $\alpha_k$  and  $\beta_k$  are coefficients independent of the  $x$ . Notice that according to Eq. 20,  $\tilde{f}(x) = f(x)$  for  $x \in [a, b]$ . Therefore, we further obtain such an essential equation as below.

$$f(x) = \tilde{f}(x) = \gamma + \sum_{k=1}^{+\infty} [\alpha_k \sin(k\omega x) + \beta_k \cos(k\omega x)] , \quad x \in [a, b] , \quad (22)$$

and the proof is finished. We intuitively show the proof method above in Figure 7.  $\square$

**Note:** According to (Zygmund & Fefferman, 2003), coefficients of the trigonometric expansion, i.e.,  $\gamma$ ,  $\alpha_k$  and  $\beta_k$ , are determined by the formulation of  $f(x)$ . Therefore, by directly replacing the constant coefficients of Eq. 10 with learnable parameters, we obtain the special graph filter  $\theta_{\text{Trigo}}$ , which can adaptively learn different kernel functions.

### A.3. Proof of Proposition 4.2

(*Vanishing coefficients*) Given a  $f(x)$  with formulation as Eq. 10, its coefficients  $\alpha_k$  and  $\beta_k$  satisfies

$$\lim_{k \rightarrow +\infty} \alpha_k = 0, \quad \lim_{k \rightarrow +\infty} \beta_k = 0. \quad (23)$$

*Proof.* The coefficients  $\alpha_k$  and  $\beta_k$  can be computed as follows:

$$\begin{aligned} \alpha_k &= \frac{\omega}{\pi} \int_0^{\frac{2\pi}{\omega}} f(x) \sin(k\omega x) dx, \\ \beta_k &= \frac{\omega}{\pi} \int_0^{\frac{2\pi}{\omega}} f(x) \cos(k\omega x) dx. \end{aligned} \quad (24)$$

We alternatively consider such a *real function*  $f'(x)$  which is defined as follows:

$$f'(x) = \begin{cases} f(x), & x \in [0, \frac{2\pi}{\omega}] ; \\ 0, & \text{others} . \end{cases} \quad (25)$$

Notice that such  $f'(x)$  satisfies the *Dirichlet conditions* (Hoskins, 2009), the *Fourier transform* of  $f'(x)$  exists according to (G.Proakis, 1975) and is defined as follows:

$$\begin{aligned} F'(\Omega) &= \int_{-\infty}^{+\infty} f'(x) e^{-i\Omega x} dx, \\ &= \int_{-\infty}^{+\infty} f'(x) [\cos(\Omega x) - i \cdot \sin(\Omega x)] dx, \end{aligned} \quad (26)$$

where  $\Omega$  denotes the variable in frequency domain, and  $i$  is the imaginary unit.

Furthermore, the  $f' \in L^1(\mathbb{R}^n)$  is an integrable function, making  $f'(x)$  satisfy the *Riemann–Lebesgue lemma* which is defined as follows:

**Theorem A.1. (Riemann–Lebesgue lemma (Bochner & Chandrasekharan, 1951)).** Let  $g \in L^1(\mathbb{R}^n)$  be an integrable function, and let  $G$  be the Fourier transform of  $g$ . Then the  $G$  vanishes at infinity, which is defined as follows:

$$\lim_{|\Omega| \rightarrow \infty} |G(\Omega)| = 0. \quad (27)$$

Thus, the limit of  $F'(\Omega)$  as  $\Omega$  approaches  $+\infty$  equals 0, which is defined as

$$\begin{aligned} \lim_{\Omega \rightarrow +\infty} F'(\Omega) &= \lim_{\Omega \rightarrow +\infty} \underbrace{\left[ \int_{-\infty}^{+\infty} f'(x) [\cos(\Omega x) - i \cdot \sin(\Omega x)] dx \right]}_{\text{Formula 1}}, \\ &= 0. \end{aligned} \quad (28)$$

Since the  $f'(x)$  is a real function, the Formula 1 equals 0 if and only if the following equations hold:

$$\begin{aligned} \lim_{\Omega \rightarrow +\infty} \int_{-\infty}^{+\infty} f'(x) \cos(\Omega x) dx &= 0, \\ \lim_{\Omega \rightarrow +\infty} \int_{-\infty}^{+\infty} f'(x) \sin(\Omega x) dx &= 0. \end{aligned} \quad (29)$$

With combing the definition of  $f'(x)$  in Eq. 25, the Eq. 29 above can be further derived as follows:

$$\begin{aligned} \lim_{\Omega \rightarrow +\infty} \int_0^{\frac{2\pi}{\omega}} f(x) \cos(\Omega x) dx &= 0, \\ \lim_{\Omega \rightarrow +\infty} \int_0^{\frac{2\pi}{\omega}} f(x) \sin(\Omega x) dx &= 0. \end{aligned} \quad (30)$$

Finally, with replacing the  $\Omega$ ,  $\Omega \rightarrow +\infty$  with  $k\omega$ ,  $k \rightarrow +\infty$  in Eq. 30, and further considering the Eq. 24, we obtain the following equations:

$$\begin{aligned}\lim_{k \rightarrow +\infty} \alpha_k &= \frac{\omega}{\pi} \cdot \lim_{k \rightarrow +\infty} \int_0^{\frac{2\pi}{\omega}} f(x) \sin(k\omega x) dx = 0, \\ \lim_{k \rightarrow +\infty} \beta_k &= \frac{\omega}{\pi} \cdot \lim_{k \rightarrow +\infty} \int_0^{\frac{2\pi}{\omega}} f(x) \cos(k\omega x) dx = 0,\end{aligned}\quad (31)$$

and the proof is completed.  $\square$

## B. Band-pass Function Approximation

In this section, we introduce experimental details of band-pass function approximation mentioned in the main paper.

### B.1. Approximation Target

To evaluate function approximation capability of different polynomials towards band-pass functions, we conduct numerical experiments in approximating 5 complicated target functions, including band-pass and the sum of band-pass type. Mathematical formulations and illustrations of these target functions are shown in Table 9 and from Figure 8b to 12b, respectively. Notably, compared to the simple target functions used in (He et al., 2021; 2022; Wang & Zhang, 2022; Guo & Wei, 2023), the target functions in this paper are more complicated with noticeably narrower pass-band, which can be regarded as linear combination of simple band-pass functions. Therefore, the numerical experiments in this paper are convincing evaluation metrics towards function approximation ability of those polynomials.

Table 9: Mathematical formulations of 5 target functions, where  $x$  satisfies  $x \in [0, 2]$ .

Function	Mathematical Formulation	Illustration
$f_1(x)$	$ \sin(\pi x) $	Figure 8b
$f_2(x)$	$\exp(-10(x-1)^2)$	Figure 9b
$f_3(x)$	$\begin{cases} 0.5 + 0.5 \cos(2\pi x), & 0 \leq x < 0.5, \\ \exp(-100(x-0.5)^2), & 0.5 \leq x < 1, \\ \exp(-100(x-1.5)^2), & 1 \leq x \leq 1.5, \\ 0.5 + 0.5 \cos(2\pi x), & 1.5 \leq x < 2. \end{cases}$	Figure 10b
$f_4(x)$	$\exp(-100(x-1.5)^2) + \exp(-100(x-0.5)^2) + 1.5 \exp(-50(x-1)^2)$	Figure 11b
$f_5(x)$	$\exp(-100x^2) + \exp(-100(x-2)^2)$	Figure 12b

### B.2. Experimental Details

**Training data generation.** To obtain the training input  $x$ , we randomly generate 50000 data points with uniform distribution on  $[0, 1]$ , and construct a 50000-dimension vector with the sorting data points, leading to significantly high resolution on the approximation target functions.

**Model Construction.** We conduct experiment on 7 polynomials (i.e., Monomial, Bernstein, Favard (Guo & Wei, 2023), Chebyshev, Jacobian, Rational and Trigonometric), which correspond to 9 relevant poly-GNNs (i.e., GPRGNN (Chien et al., 2021), BernNet (He et al., 2021), OptBasis (Guo & Wei, 2023), ChebNetII (He et al., 2022), JacobiConv (Wang & Zhang, 2022), CayleyNet (Levie et al., 2019), ARMA (Bianchi et al., 2020) and our TrigoNet). To make experimental evaluation on polynomials consistent to empirical studies on relevant poly-GNNs, we follow the construction techniques used in relevant models to conduct model for each polynomial. The polynomial order is set 10 for conventional cases, (10, 10) is set for rational one, and the Taylor expansion order for trigonometric polynomial is optimized over  $\{4, 6, 8, 10\}$ .

**Optimization and Evaluation.** We perform the numerical experiment as an intuitive regression problem with squared loss  $\sum_{n=1}^{50000} [T_K(x_n; \xi) - f_i(x_n)]^2$ , and use Adam optimizer (Kingma & Ba, 2014) with weight decay=0 and learning rate= $5e-4$  to optimize the model in 2000 epochs. Thus, the squared loss of the trained model can be regarded as an intuitive evaluation metric to the function approximation capability of the corresponding polynomial. Furthermore, to tackle the bias

caused by irrelevant factors, e.g., random seeds, and achieve fair evaluation, we repeat the numerical experiment 20 times and take the average loss as the final evaluation metric for each polynomial.

### B.3. Results

Similar to Figure 2, in Figure 8, 9, 10, 11 and 12, we present full experimental results of 7 polynomials on all 5 band-pass functions. As clearly shown in these figures, the trigonometric polynomial achieved substantial performance on band-pass functions approximation, while its approximation error is slightly higher than rational polynomial but noticeably lower than conventional polynomials. According to our analysis in the main paper, these substantial results empirically demonstrate the effectiveness of our method to some extent.

## C. Experimental Details

In this section, we provide extensive details towards the experiments in Section 5.

### C.1. Datasets Statistics

We summarize the datasets statistics in Table 10. For the 9 small- and middle-scaled datasets, we follow (Chien et al., 2021; He et al., 2021; 2022; Wang & Zhang, 2022; Guo & Wei, 2023) to randomly divide the node set into train/test/val with ratio 60%/20%/20%; for the OGB datasets, we use the standard nodes split proposed in the original OGB datasets’ paper (Hu et al., 2020).

Table 10: Datasets statistics.

	Cora	CiteSeer	PubMed	Computers	Photo	Chameleon	Squirrel	Texas	Cornell	Ogbn-arxiv	Ogbn-Papers100M
Nodes	2708	3327	19,717	13,752	7650	2277	5201	183	183	169,343	111,059,956
Edges	5278	4552	44,324	245,861	119,081	31,371	198,353	279	277	1,166,243	1,615,685,872
Features	1433	3703	500	767	745	2325	2089	1703	1703	128	128
Classes	7	6	5	10	8	5	5	5	5	40	172

### C.2. Node Classification on Small- and Middle-scale Datasets

We provide experimental details to the experiments in Section 5.1.

**Baselines.** For GCN, ARMA, ChebNet and APPNP, we use Pytorch Geometric (Fey & Lenssen, 2019) implementations following (He et al., 2022). For other baselines, we use publicly released implementations as follows.

- **IGCN:** <https://github.com/liqimai/Efficient-SSL>
- **CayleyNet:** <https://github.com/amoliu/CayleyNet>
- **GPRGNN:** <https://github.com/jianhao2016/GPRGNN>
- **BernNet:** <https://github.com/ivam-he/BernNet>
- **JacobiConv:** <https://github.com/GraphPKU/JacobiConv>
- **ChebNetII:** <https://github.com/ivam-he/ChebNetII>
- **OptBasis:** <https://github.com/yuziGuo/FarOptBasis>

**Hyper-parameter settings.** We follow the same settings on model paradigms as the original papers for the rest baselines except for GCN, ARMA, ChebNet and APPNP, while we follow the same settings as (He et al., 2021; 2022; Wang & Zhang, 2022; Guo & Wei, 2023) for the rest 4 baselines. For our TrigoNet, motivated by the Proposition 4.2, we turn to optimize the  $\omega$ , the product  $K \cdot \omega$ , and interval  $K - K^*$  instead of optimizing the  $K$ ,  $K^*$  and  $\omega$  separately, which significantly simplifies the optimization procedure. Specifically, we optimize the  $K \cdot \omega$  over  $\{\pi, 1.1\pi, 1.2\pi, \dots, 2.4\pi, 2.5\pi\}$ , the  $\omega$  over  $\{0.05\pi, 0.1\pi, 0.2\pi, 0.3\pi, 0.4\pi, 0.5\pi, 0.7\pi, 0.9\pi\}$ , the  $K - K^*$  over  $\{1, 2, 3, 4, 5, 6\}$ , and the Taylor expansion order over  $\{4, 6, 8, 10\}$ .

For all models, we optimize the common hyper-parameters, i.e., weight decay, learning rate and dropout rate, with grid search over the same large search ranges for fairness, while the search ranges are shown in Table 11.

Table 11: Search ranges of common hyper-parameters.

Parameter	Search Ranges
weight decay	$\{0, 1e-7, 5e-7, 1e-6, 5e-6, \dots, 1e-1, 5e-1\}$
learning rate	$\{5e-2, 2e-2, 1e-2, \dots, 5e-4, 2e-4, 1e-4\}$
dropout rate	$\{0, 0.1, 0.2, 0.3, \dots, 0.7, 0.8, 0.9\}$

### C.3. Node Classification on Large-scale Datasets

We provide experimental details to the experiments in Section 5.2.

**Baselines.** For the experiments on large graphs, we further introduce 3 baselines specially designed for learning on large graphs, i.e., SIGN, GBP and NDLS, while the implementations are taken from released code as follows.

- **SIGN** <https://github.com/twitter-research/sign>
- **GBP** <https://github.com/chennnM/GBP>
- **NDLS** <https://github.com/zwt233/NDLS>

**Hyper-parameter settings.** For all baselines, we follow the same model settings used in (He et al., 2022; Guo & Wei, 2023). For our TrigoNet, we optimize the  $K$ ,  $K^*$  and  $\omega$  with the same parameter search ranges and optimization strategy as Appendix C.2. As mentioned in Section 5.2, an MLP is used in TrigoNet, making our method achieve the same model paradigm as GPRGNN, BernNet, ChebNetII and OptBasis. We follow (He et al., 2022; Guo & Wei, 2023) to tune the hyper-parameters for each MLP layer individually with the same large search ranges as Appendix C.2.

## D. Full Results of Ablation Studies

In this section, we present more extensive results of ablation studies towards  $\omega$ ,  $K$  and  $K^*$ .

**Full Ablation Studies towards  $\omega$  and  $K$ .** Similar to Figure 5, we show the sensitivity map of model performance towards  $(\omega, K)$  on all benchmark datasets in Figure 13, Figure 14 and Figure 15. As shown in these figures, we further empirically verify the rationality and correctness of our analysis in Section 5.3, which demonstrates robustness of both  $\omega$  and  $K$ .

**Full Ablation Studies towards  $K^*$ .** Similar to Figure 6, we show the effect of  $K^*$  towards model performance on all benchmark datasets in Figure 16, Figure 17 and Figure 18. As shown in these figures, we further empirically verify our analysis in Section 5.3, which demonstrates the correctness of Proposition 4.2 and Eq. 11.

## E. Related Works

### E.1. Polynomial Approximation

Polynomial approximation (Smyth, 1998; Phillips, 2003) is a technique that uses the sum of polynomial to achieve approximate construction of some complicated (or unachievable) functions (Funaro, 2008), or to solve an interpolation problems with given function nodes (De Boor & Ron, 1990; Gasca & Sauer, 2000), while both similarly focus on involving well-defined polynomial into obtaining truncated polynomial approximation to the target functions.

The polynomial used for approximation is formulated with an unique basis function that determines special property of this polynomial. For instance, the polynomial with its basis orthogonal on domain, e.g., Chebyshev polynomial (Rivlin, 2020) and Jacobian polynomial (Szeg, 1939), is called orthogonal polynomial (Szeg, 1939; Chihara, 2011) which maintains orthogonality that leads to superior computational advantages in function approximation; Bernstein polynomial (Lorentz, 2013) involves non-negative and non-orthogonal Bernstein basis, making it an ideal polynomial for constructing non-negative functions (Papp & Alizadeh, 2014); Rational polynomial (Newman, 1979; Litvinov, 2001; Mason, 2006; Popov, 2011; Achieser, 2013) is a fraction such that both numerator and denominator are polynomials, leading to more generalized form of

polynomial; Trigonometric polynomial (Sharma & Varma, 1965; Zygmund & Fefferman, 2003) involves trigonometric basis function into conducting approximation on  $(-\infty, +\infty)$ , making it an ideal choice for approximating periodic functions and band-pass functions (Taubin et al., 1996; Fu & Willson, 1999; Davidson et al., 2002; Gudino et al., 2008; Zahradnik & Vlcek, 2012; Zhao & Tay, 2023). Notably, since each polynomial has special properties associated with its basis function, the selection of polynomial for approximation should be problem-oriented instead of universal.

## E.2. Polynomial-based Spectral GNNs

Spectral GNNs with polynomial-based graph filters have achieved significant results on graph learning tasks, especially node classification. Compared to those involving graph filters with fixed mathematical formulations, e.g., GCN (Kipf & Welling, 2017), these polynomial-based spectral GNNs adaptively construct ad-hoc graph filter for each dataset with polynomial approximation, leading to more flexible and efficient paradigm of spectral GNNs.

For instance, ChebNet (Defferrard et al., 2016) constructs graph filter with Chebyshev polynomial (Rivlin, 2020); GPRGNN (Chien et al., 2021) performs graph convolution as the sum of  $K$ -order propagation, which can be regarded as spectral graph filter with Monomial polynomial; BernNet (He et al., 2021) constructs non-negative graph filter-bank through applying Bernstein polynomial (Lorentz, 2013); through involving Chebyshev nodes (Rivlin, 2020; Smyth, 1998; Phillips, 2003) into polynomial approximation, (He et al., 2022) proposes an improved ChebNet named ChebNetII; JacobiConv (Wang & Zhang, 2022) constructs graph filter with Jacobian polynomial (Szeg, 1939) and deserts nonlinearity, leading to an effective model with noticeable efficiency; instead of applying specific polynomial, OptBasis (Guo & Wei, 2023) proposes a learnable polynomial base for adaptive filter construction, leading to substantial model flexibility; CayleyNet (Levie et al., 2019) uses Jacobian iteration to obtain approximate construction of the cayley filter; (Bianchi et al., 2020) proposes a stacking GNN block based on the ARMA filter, leading to an approximate rational polynomial spectral GNN.

## F. Visualization of Learned Graph Filters

Similar to previous works (He et al., 2021; Li et al., 2022; He et al., 2022; Wang & Zhang, 2022), from Figure 19 to Figure 29, we visualize the graph filters learned with TrigoNet on each dataset, where the graph filters achieved on each frequency are shown respectively. Moreover, the figures intuitively show that filters learned by TrigoNet are generally band-pass or the sum of band-pass, indicating the correctness of our statement in Section 3.

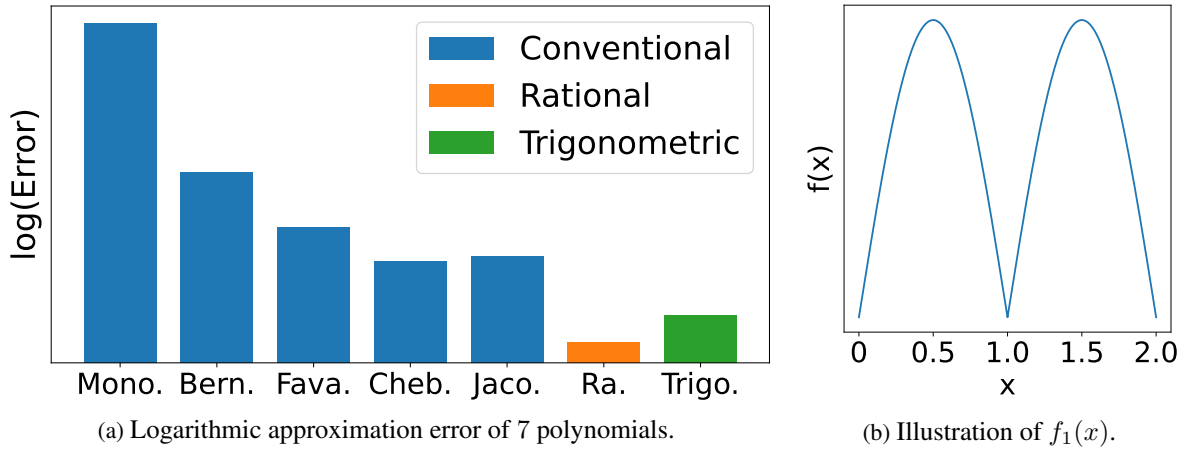


Figure 8: Logarithmic approximation error to  $f_1(x)$ .

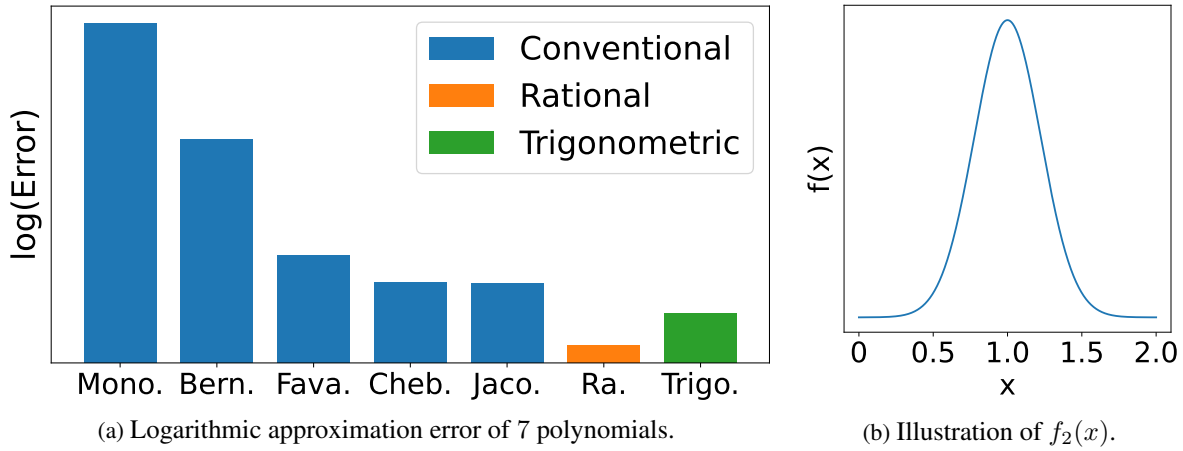


Figure 9: Logarithmic approximation error to  $f_2(x)$ .

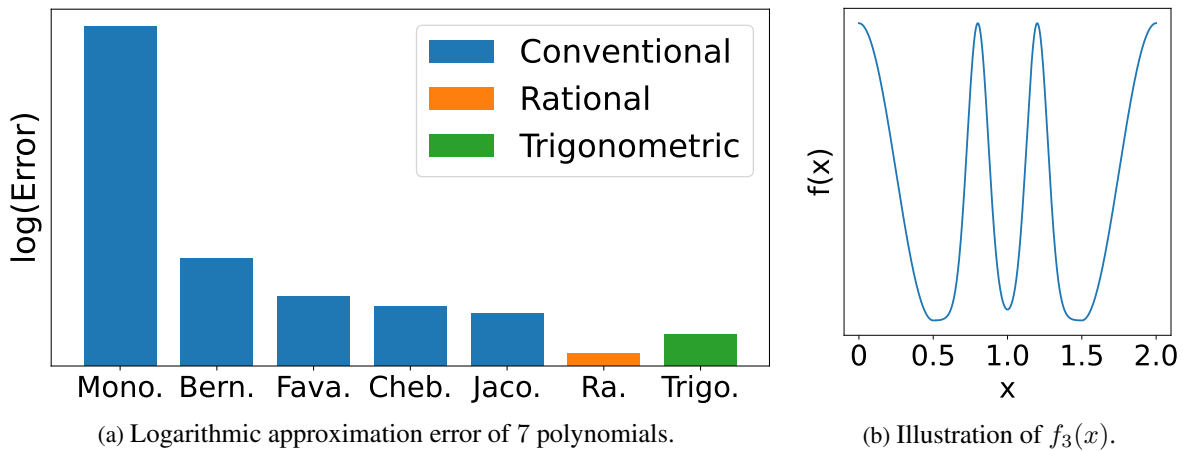


Figure 10: Logarithmic approximation error to  $f_3(x)$ .

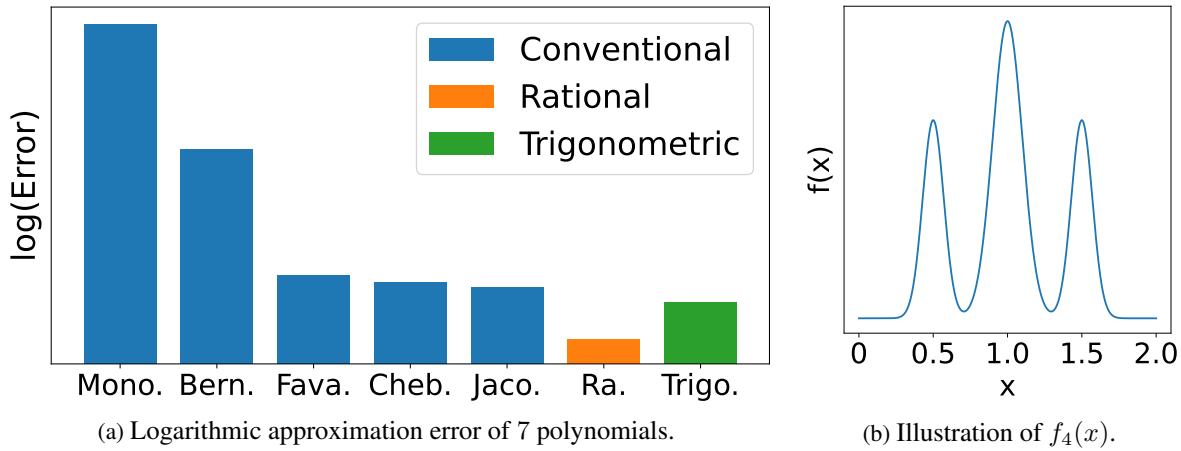


Figure 11: Logarithmic approximation error to  $f_4(x)$ .

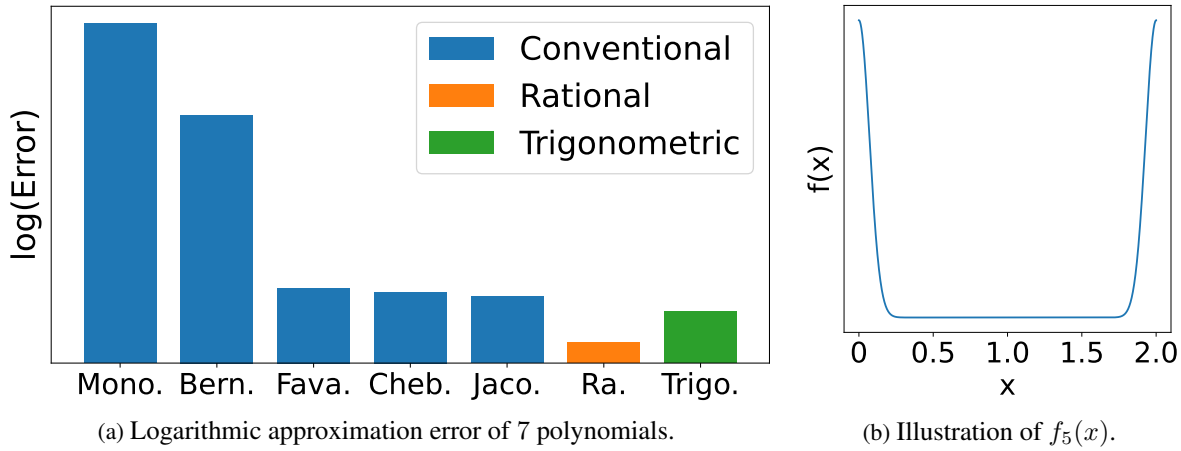


Figure 12: Logarithmic approximation error to  $f_5(x)$ .

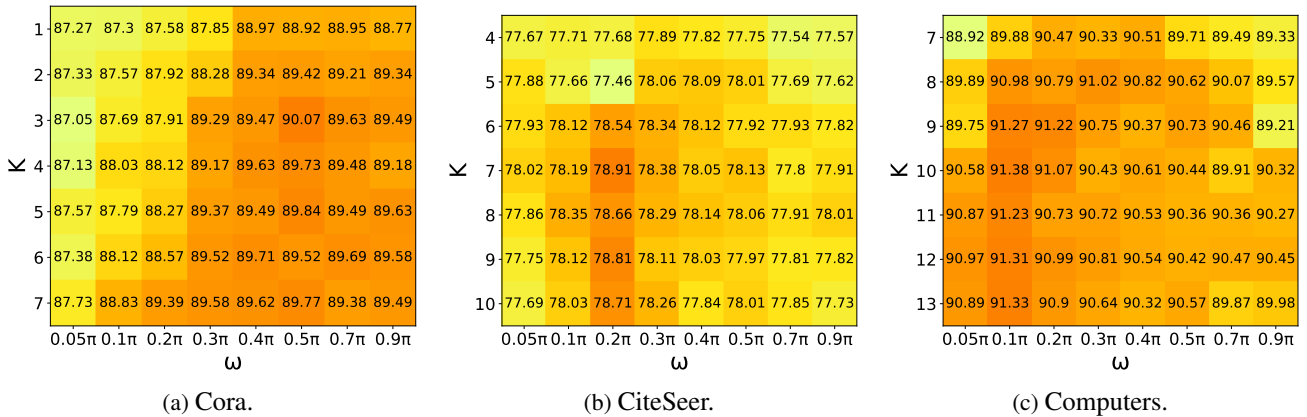


Figure 13: Parametric sensitivity analysis of  $\omega$  and  $K$  on Cora, CiteSeer and Computers.

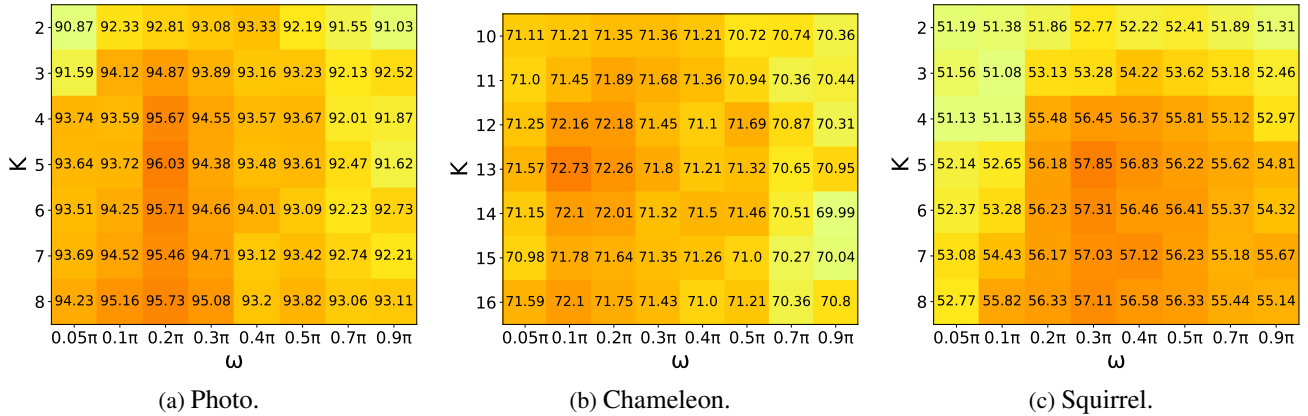


Figure 14: Parametric sensitivity analysis of  $\omega$  and  $K$  on Photo, Chameleon and Squirrel.

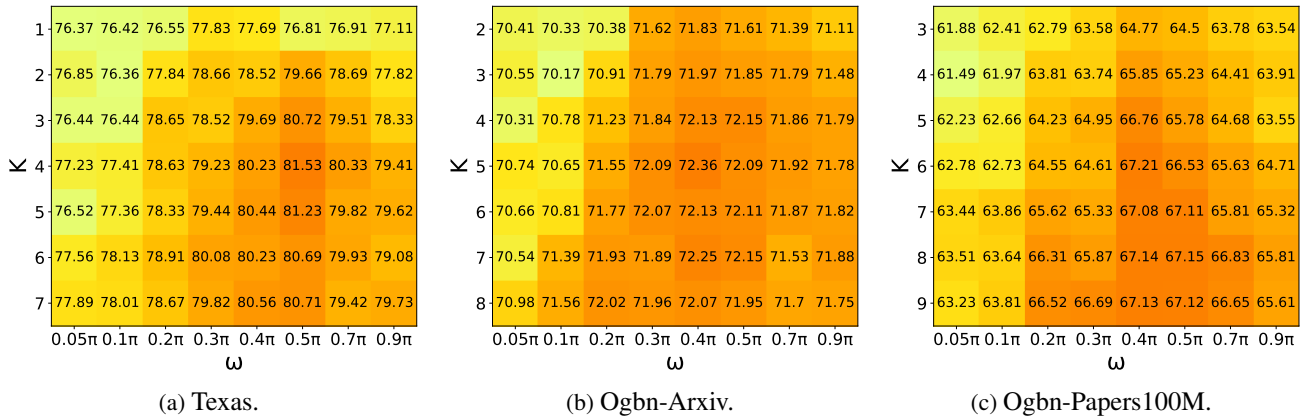


Figure 15: Parametric sensitivity analysis of  $\omega$  and  $K$  on Texas, Ogbn-Arxiv and Ogbn-Papers100M.

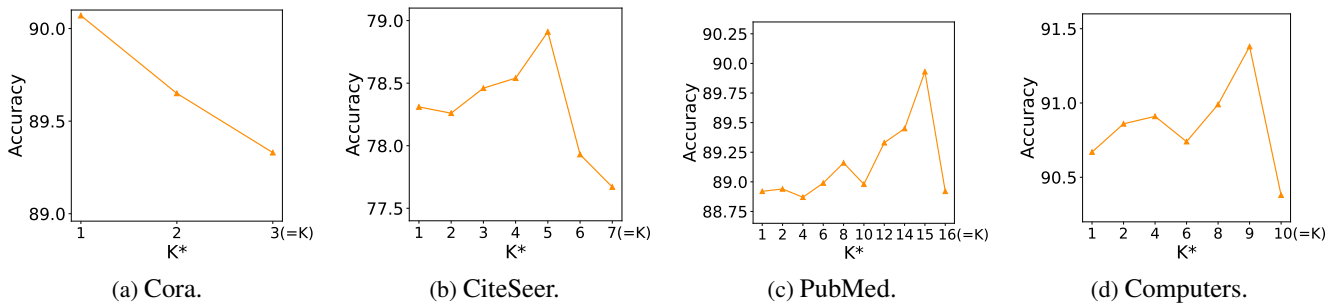


Figure 16: Effect of  $K^*$  towards model performance on Cora, CiteSeer, PubMed and Computers.

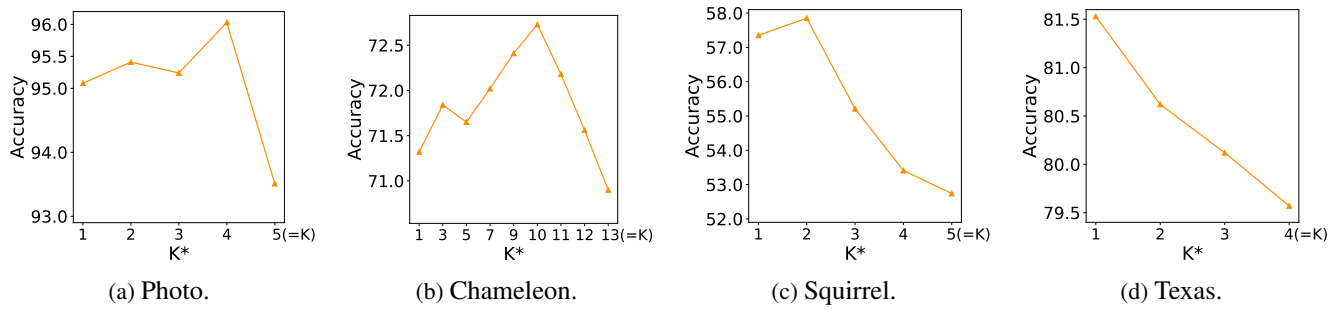


Figure 17: Effect of  $K^*$  towards model performance on Photo, Chameleon, Squirrel and Texas.

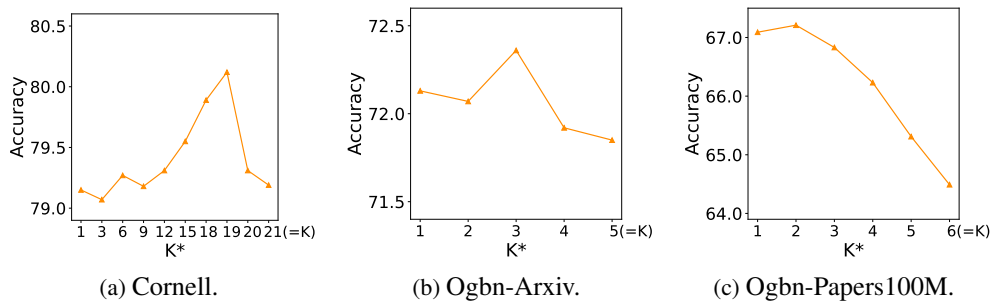


Figure 18: Effect of  $K^*$  towards model performance on Cornell, Ogbn-Arxiv and Ogbn-Papers100M.

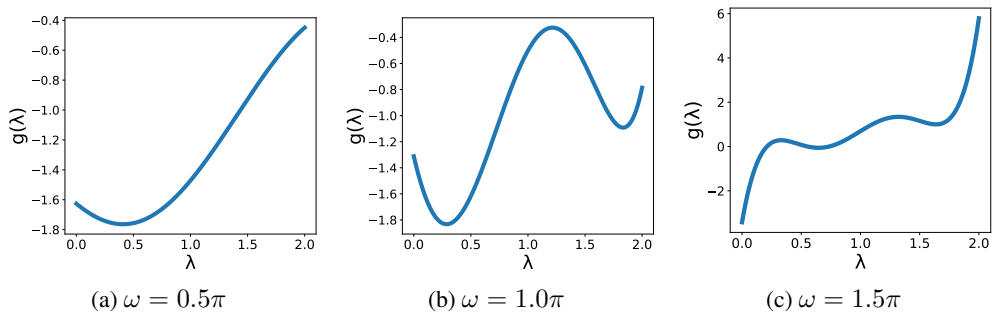


Figure 19: Learned graph filters on Cora.

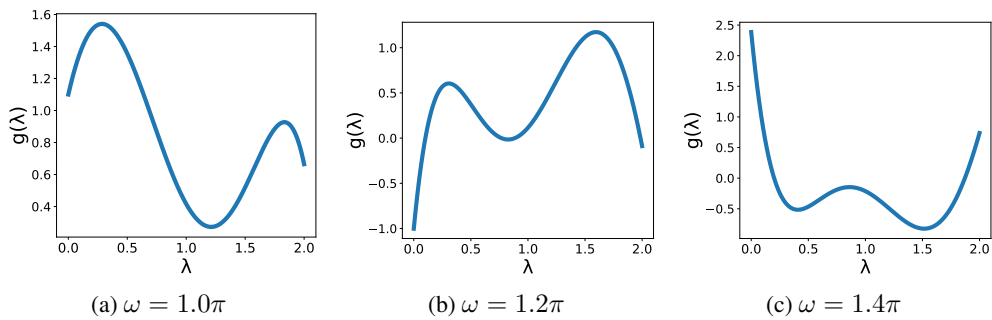


Figure 20: Learned graph filters on CiteSeer.

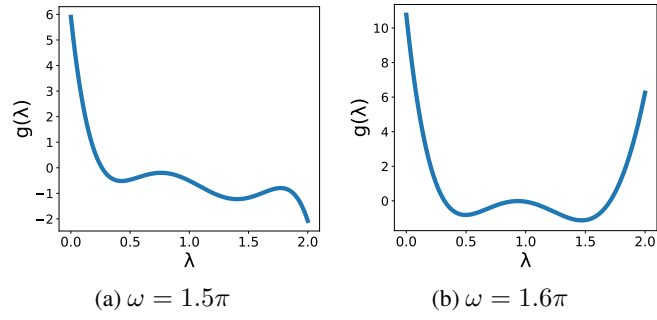


Figure 21: Learned graph filters on PubMed.

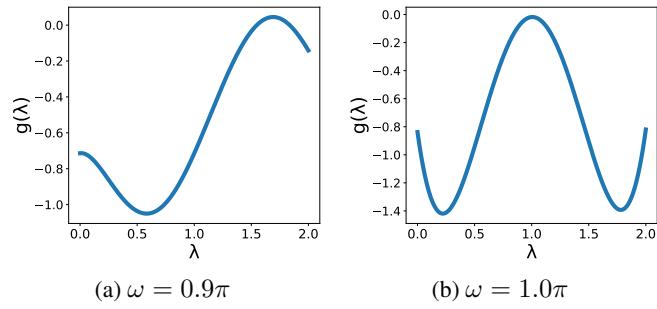


Figure 22: Learned graph filters on Computers.

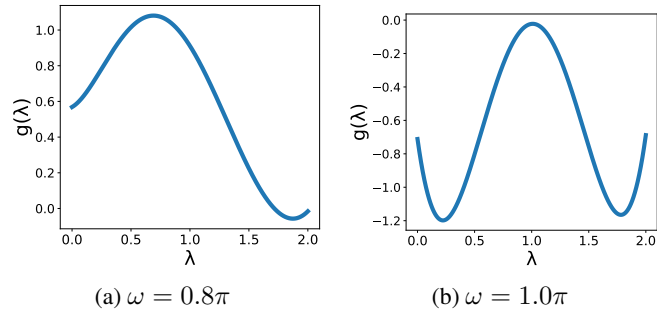


Figure 23: Learned graph filters on Photo.

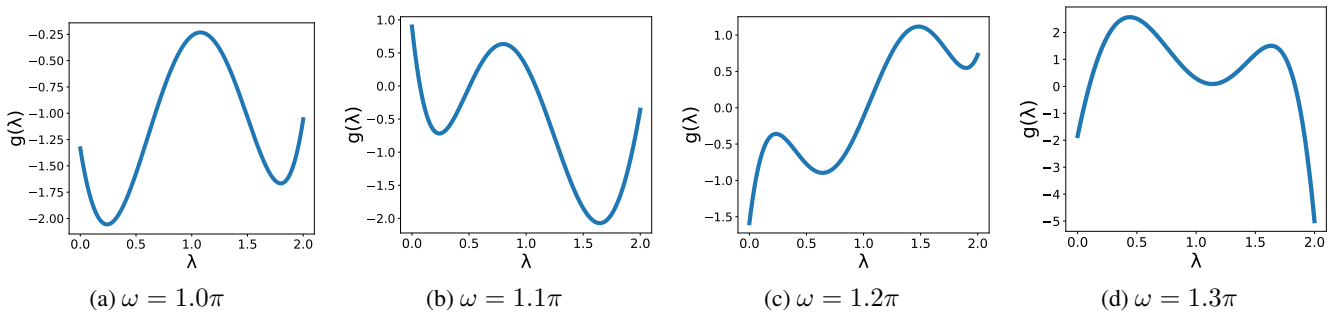


Figure 24: Learned graph filters on Chameleon.

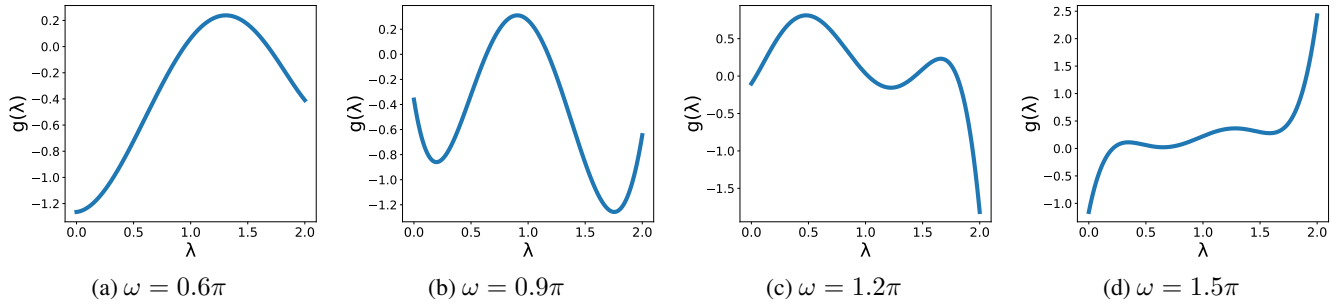


Figure 25: Learned graph filters on Squirrel.

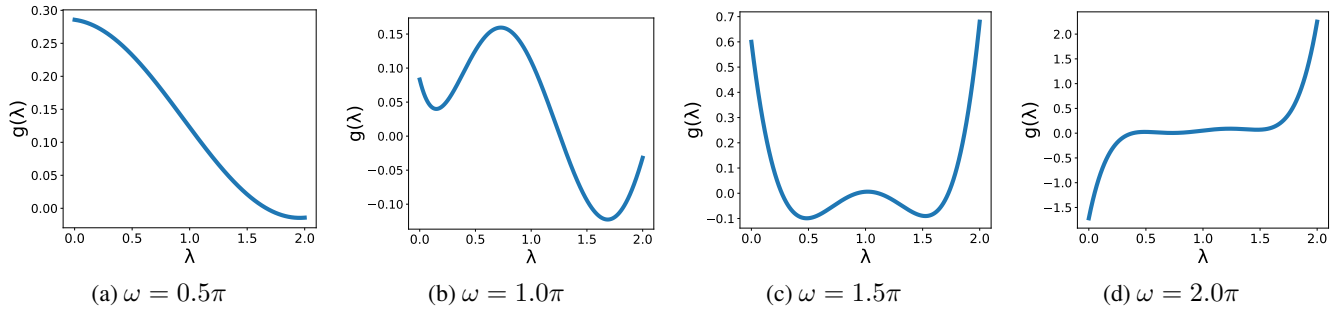


Figure 26: Learned graph filters on Texas.

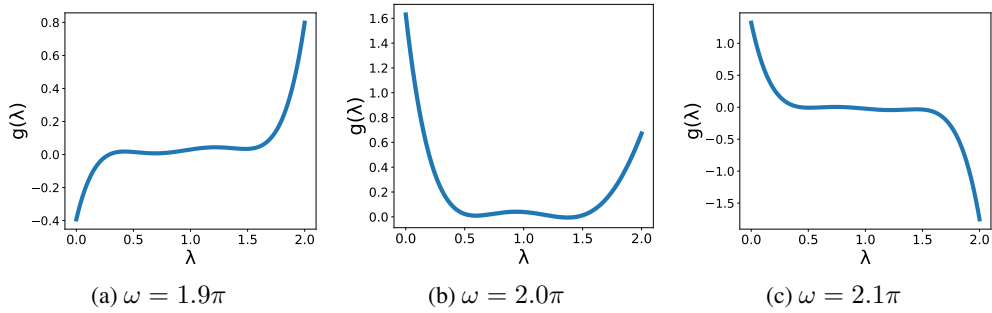


Figure 27: Learned graph filters on Cornell.

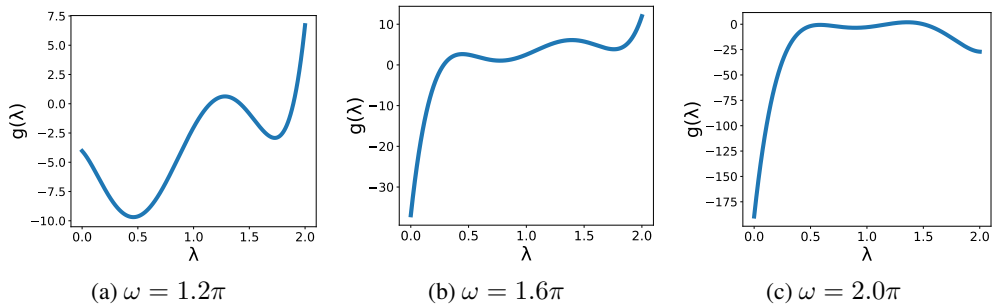


Figure 28: Learned graph filters on Ogbn-Arxiv.

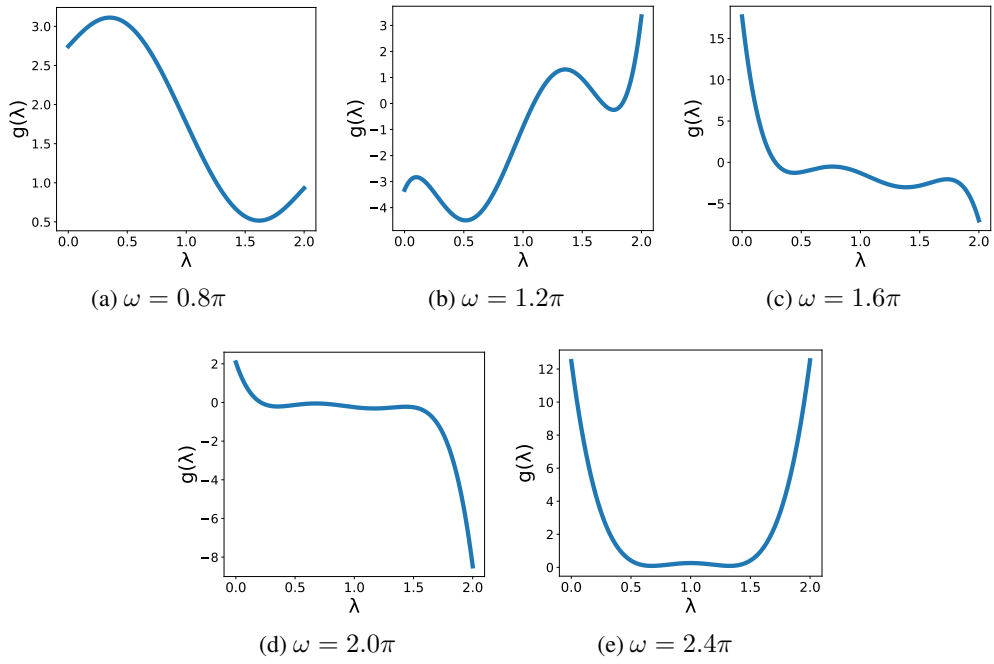


Figure 29: Learned graph filters on Ogbn-Papers100M.